JPL PUBLICATION 77-83

Evaluation of Landsat MSS vs TM Simulated Data for Distinguishing "Hydrothermal Alteration"

National Aeronautics and
Space Administration

Jet Propulsion Laboratory
California Institute of Technology
Pasadena, California 91103

JPL PUBLICATION 77-83

Evaluation of Landsat MSS vs TM Simulated Data for Distinguishing "Hydrothermal Alteration"

Michael J. Abrams
Anne B. Kahle
Daryl P. Madura
James M. Soha

March 1, 1978

National Aeronautics and
Space Administration

Jet Propulsion Laboratory
California Institute of Technology
Pasadena, California 91103

PREFACE

The work described herein was performed by the Earth and Space Sciences Division of the Jet Propulsion Laboratory.

ABSTRACT

The object of this study was to simulate Landsat Follow-On (LFO) data to demonstrate the mineral exploration capability of this prospective system for segregating different types of hydrothermal alteration and to compare this capability with that of the existing Landsat system.

Multispectral data were acquired for several test sites with the Bendix 24-channel MSDS scanner. This instrument had spectral bands closely approximating those of the LFO. The data were geometrically corrected, noise was removed, and resolution was degraded to LFO parameters prior to further computer processing. Contrast enhancements, band ratioing, and principal component transformations were used to process the simulated LFO data for analysis.

For the Red Mountain, Arizona, test area, the LFO data allowed identification of silicified areas, not identifiable with Landsat 1 and 2 data. In addition, the improved LFO resolution allowed detection of small silicic outcrops and of a narrow silicified dike. For the Cuprite - Ralston, Nevada, test area, the LFO spectral bands allowed discrimination of argillic and opalized altered areas; these could not be spectrally discriminated using Landsat 1 and 2 data. Addition of data from the 1.3- and 2.2-μm regions allowed better discriminations of hydrothermal alteration types.

TECHNICAL REPORT STANDARD TITLE PAGE

1. Report No. JPL Pub. 77-83	2. Government Accession No.	3. Recipient's Catalog No.
4. Title and Subtitle Evaluation of Landsat MSS vs TM Simulated Data for Distinguishing "Hydrothermal Alternation"		5. Report Date March 1, 1978 6. Performing Organization Code
7. Author(s) M.J. Abrams/A. B. Kahle/D.P. Madura/J.M. Soha		8. Performing Organization Report No.
9. Performing Organization Name and Address JET PROPULSION LABORATORY California Institute of Technology 4800 Oak Grove Drive Pasadena, California 91103		10. Work Unit No. 11. Contract or Grant No. NAS 7-100 13. Type of Report and Period Covered JPL Publication
12. Sponsoring Agency Name and Address NATIONAL AERONAUTICS AND SPACE ADMINISTRATION Washington, D.C. 20546		14. Sponsoring Agency Code

15. Supplementary Notes

16. Abstract

The ~~objective of this study was to~~ simulate Landsat Follow-On (LFO) data to demonstrate the mineral exploration capability of this prospective system for segregating different types of hydrothermal alteration and to compare this capability with that of the existing Landsat system.

Multispectral data were acquired for several test sistes with the Bendix 24-channel MSDS scanner. This instrument had spectral bands closely approximating those of the LFO. The data were geometrically corrected, noise was removed, and resolution was degraded to LFO parameters prior to further computer processing. Contrast enhancements, band ratioing, and principal component transformations were used to process the simulated LFO data for analysis.

For the Red Mountain, Arizona, test area, the LFO data allowed identification of silicified areas, not identifiable with Landsat 1 and 2 data. In addition, the improved LFO resolution allowed detection of small silicic outcrops and of a narrow silicified dike. For the Cuprite-Ralston, Nevada, test area, the LFO spectral bands allowed discrimination fo argillic and opalized altered areas; these could not be spectrally discriminated using Landsat 1 and 2 data. Addition of data from the 1.3- and 2.2-μm regions allowed better discriminations of hydrothermal alteration types.

17. Key Words (Selected by Author(s))	18. Distribution Statement
Geosciences (General) Earth Resources	Unclassified – Unlimited

19. Security Classif. (of this report)	20. Security Classif. (of this page)	21. No. of Pages	22. Price
Unclassified	Unclassified	56	

HOW TO FILL OUT THE TECHNICAL REPORT STANDARD TITLE PAGE

Make items 1, 4, 5, 9, 12, and 13 agree with the corresponding information on the report cover. Use all capital letters for title (item 4). Leave items 2, 6, and 14 blank. Complete the remaining items as follows:

3. Recipient's Catalog No. Reserved for use by report recipients.

7. Author(s). Include corresponding information from the report cover. In addition, list the affiliation of an author if it differs from that of the performing organization.

8. Performing Organization Report No. Insert if performing organization wishes to assign this number.

10. Work Unit No. Use the agency-wide code (for example, 923-50-10-06-72), which uniquely identifies the work unit under which the work was authorized. Non-NASA performing organizations will leave this blank.

11. Insert the number of the contract or grant under which the report was prepared.

15. Supplementary Notes. Enter information not included elsewhere but useful, such as: Prepared in cooperation with... Translation of (or by)... Presented at conference of... To be published in...

16. Abstract. Include a brief (not to exceed 200 words) factual summary of the most significant information contained in the report. If possible, the abstract of a classified report should be unclassified. If the report contains a significant bibliography or literature survey, mention it here.

17. Key Words. Insert terms or short phrases selected by the author that identify the principal subjects covered in the report, and that are sufficiently specific and precise to be used for cataloging.

18. Distribution Statement. Enter one of the authorized statements used to denote releasability to the public or a limitation on dissemination for reasons other than security of defense information. Authorized statements are "Unclassified—Unlimited," "U. S. Government and Contractors only," "U. S. Government Agencies only," and "NASA and NASA Contractors only."

19. Security Classification (of report). NOTE: Reports carrying a security classification will require additional markings giving security and downgrading information as specified by the Security Requirements Checklist and the DoD Industrial Security Manual (DoD 5220.22-M).

20. Security Classification (of this page). NOTE: Because this page may be used in preparing announcements, bibliographies, and data banks, it should be unclassified if possible. If a classification is required, indicate separately the classification of the title and the abstract by following these items with either "(U)" for unclassified, or "(C)" or "(S)" as applicable for classified items.

21. No. of Pages. Insert the number of pages.

22. Price. Insert the price set by the Clearinghouse for Federal Scientific and Technical Information or the Government Printing Office, if known.

CONTENTS

Tables

SECTION I

INTRODUCTION

The object of this study was to simulate Landsat Follow-On (LFO) data in order to demonstrate the mineral exploration capability of this prospective satellite system and compare this capability to that of the Landsat 1 and 2 systems. The effort was concentrated on identifying and separating types of hydrothermal alteration associated with base metal deposits. It was expected that better results should be achievable using the Landsat Follow-On system than are now realized with Landsat 1 and 2, due to (1) a better choice of spectral bands and (2) increased spatial resolution.

The approach taken was to simulate Landsat Follow-On data with high-resolution multispectral data acquired with the Bendix 24-channel scanner flown on NASA's NC-130 aircraft. Aircraft data in the spectral bands most closely matching the bands proposed for Landsat Follow-On and degraded in spatial resolution to match the expected Landsat Follow-On data were used as the basic data for this study. These data were computer-enhanced by the same techniques currently being applied to Landsat 1 and 2 data. A comparison was made between the enhanced processed aircraft data and enhanced Landsat 1 and 2 images for the same areas. The areas chosen for the study were those where previous geologic field work with JPL's portable field reflectance spectrometer (PFRS) had established the desirability of having multispectral data in wavelengths other than those available on Landsat 1 and 2.

Of particular interest to this study were the additional bands centered at 1.6 and 2.2 μm. These are the channels which statistical studies of field-acquired spectral data had indicated should be most useful for the separation of hydrothermal-altered rocks from unaltered rocks. This separation had yet to be demonstrated with scanner image data.

SECTION II

ACQUISITION OF DATA

The Bendix MSDS 24-channel scanner was chosen as the aircraft instrument to provide the primary data set because it has wavelength channels similar to those proposed for Landsat Follow-On. A brief description of this scanner is given in the Johnson Space Center Earth Resources Aircraft Plan (1975, Ref. 2-1), and this description is reproduced here in Table 2-1. Table 2-2 lists the wavelength channels of Landsats 1, 2, C, the proposed channels for Landsat Follow-On, and the comparable channels on the MSDS.

Data from the 24-channel scanner flown aboard the NASA NC-130 aircraft were acquired over test sites at Red Mountain, Arizona; Goldfield, Nevada; and Tintic, Utah, in November 1975. The data were of rather poor quality, with considerable noise and with data from some of the important channels missing completely. Therefore a second set of data was acquired on June 14, 1975, at Goldfield, Tintic and Battle Mountain, Nevada. These data were of improved quality, with all bands operational in the first three arrays. However, because of time constraints and because of the uncertainty of acquiring the second set of flights, considerable effort was spent on analysis of the first data set in the period between the two flights.

The geographical coordinates of the flight lines are given in Table 2-3, and the dates of the flights in Table 2-4. Location maps of the two principal test sites chosen for analysis in this study are given in Figs. 2-1, 2-2, and 2-3.

Table 2-1. Multispectral Scanner (MSDS)

(An electro-optical system which records simultaneously in 24 discrete spectral channels covering a dynamic range from 0.34 μm to 13 μm)

Spectral Characteristics

Array Number	Channel Number	Bandwidth, μm	Detector	Array Number	Channel Number	Bandwidth, μm	Detector
0	1	0.34-0.4	Photomultiplier	3	13	2.1-2.36	
	2	0.4-0.44	Photomultiplier		14	3.54-4.0	InSb
	3	0.46-0.5	Photomultiplier		15	4.5-4.75	InSb
1	4	0.53-0.57	Si	4	16	6.0-7.0	Hg-doped Ge
	5	0.57-0.63	Si		17	8.3-8.8	Hg-doped Ge
	6	0.64-0.68	Si		18	8.8-9.3	Hg-doped Ge
	7	0.71-0.75	Si		19	9.3-9.8	Hg-doped Ge
	8	0.76-0.80	Si		20	10.1-11.0	Hg-doped Ge
	9	0.82-0.87	Si		21	11.0-12.0	Hg-doped Ge
	10	0.97-1.05	Si		22	12.0-13.0	Hg-doped Ge
2	11	1.18-1.30	Ge	2	23	1.12-1.16	Ge
	12	1.52-1.73	Ge	1	24	1.05-1.09	Si

Spatial characteristics: scan angle, ±40 deg; IFOV, 2 mrad.
Physical parameters measured: records reflected and emitted energy in spectral bands between 0.34 μM and 13.0 μm.
Applications: soil characteristics, plant vigor and disease, mineral identification, water and air pollution, ocean water productivity.
Manufacturer: Bendix Aerospace.
Cost: $6,600,000 including data analysis station (DAS).
Date manufactured/obtained: August 1971.
Aircraft platform: NC130B.
Current performance: fair (major problems arrays 3 and 4).
Remarks: (1) Complex system and difficult to maintain.
(2) Imposes large load to data processing capability.

Table 2-2. Landsat Wavelength Channels, μm
(excluding thermal)

Landsat 1, 2, C	Landsat D	MSDS	
	.45-.52	3	.46-.50
.5-.6	.52-.60	4	.53-.57
.6-.7	.63-.69	6	.64-68
.7-.8	.76-.90	8	.76-.80
		9	.82-.87
.8-1.1	1.0-1.3[a]	11	1.18-1.30
	1.55-1.75	12	1.52-1.73
	2.08-2.35[a]	13	2.10-2.36

[a] Proposed.

Table 2-3. Test Sites

Site		Flight Line			
No.	Name	No.	Latitude/Longitude	Latitude/Longitude	Length, nm
030	Red Mountain, Arizona	1	31°35.9'N/110°51.3'W	31°25.7'N/110°40.0'W	14
		2	31°37.5'N/110°49.4'W	31°27.3'N/110°37.5'W	14
				Total	28
075	Goldfield, Nevada	1	37°48.0'N/117°13.6'W	37°30.0'N/117°13.6'W	18
		2	37°48.0'N/117°10.4'W	37°30.0'N/117°10.4'W	18
		3	37°59.0'N/117°52.0'W	37°57.0'N/117°59.0'W	6
				Total	42
005	Tintic District, Utah	1	39°52.0'N/112°09.0'W	40°04.0'N/112°09.0'W	12
		2	39°52.0'N/112°06.0'W	40°04.0'N/112°06.0'W	12
		3	39°52.0'N/112°03.0'W	40°04.0'N/112°03.0'W	12
				Total	36
021	Battle Mountain, Nevada	1	40°27.0'N/116°41.0'W	40°13.0'N/116°45.0'W	14
				Total	14

Table 2-4. Flight Dates

	Site	Dates Flown	
030	Red Mountain, Arizona	11-14-75	
075	Goldfield, New York	11-06-75	06-14-76
		11-13-75	
005	Tintic District, Utah	11-04-75	06-14-76
021	Battle Mountain, Nevada		06-14-76

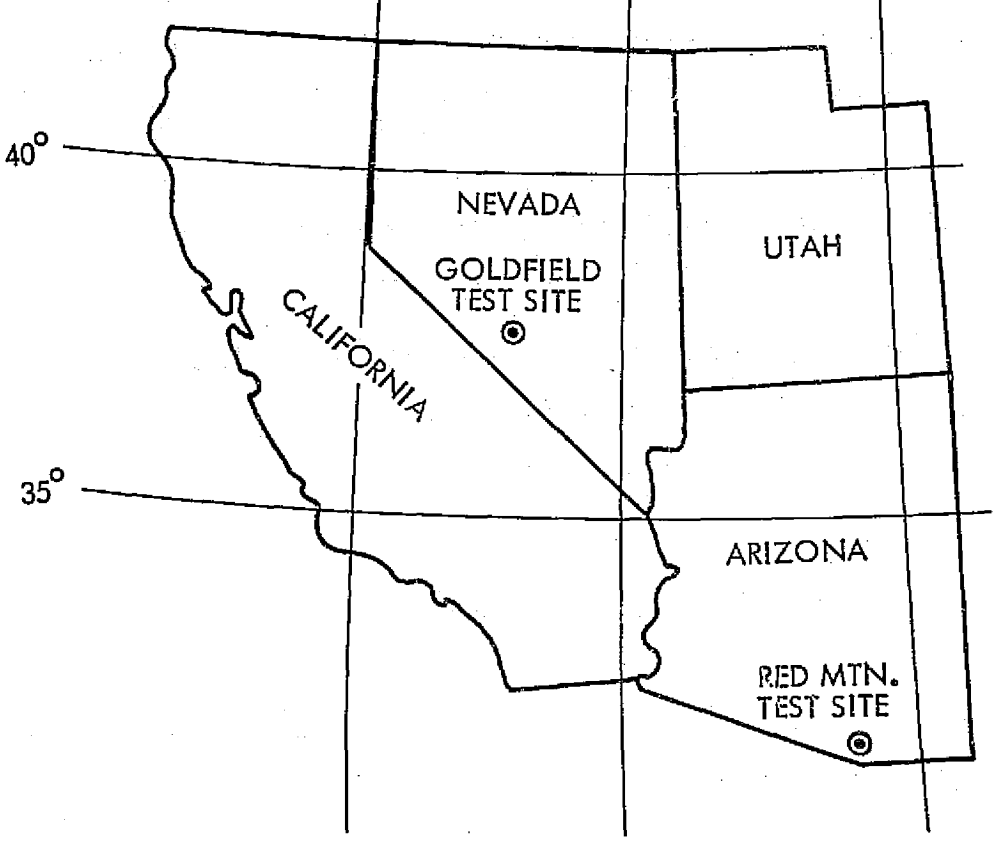

Figure 2-1. Location Map of Test Areas

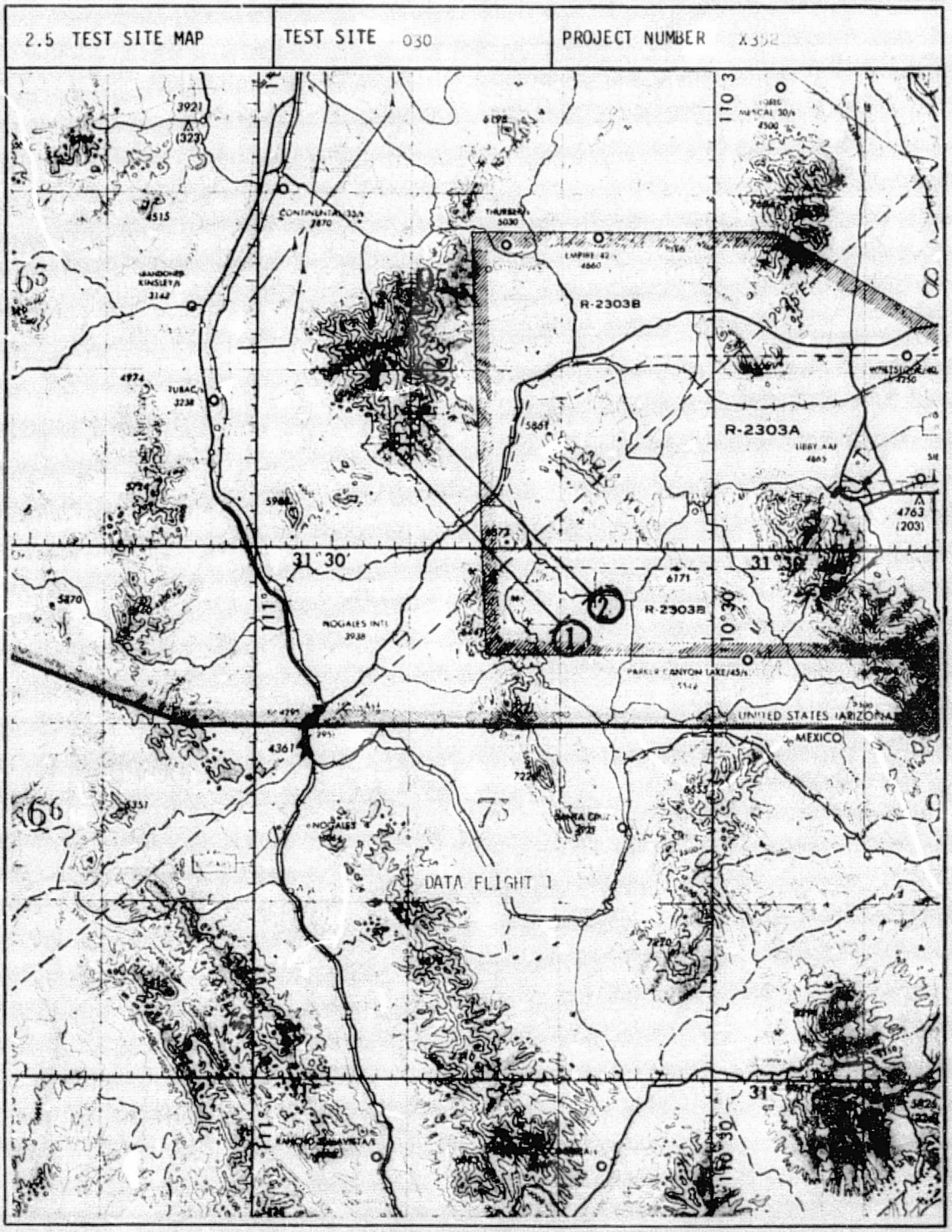

Figure 2-2. Red Mountain Flight Line

2.5 TEST SITE MAP	TEST SITE 075	PROJECT NUMBER X352

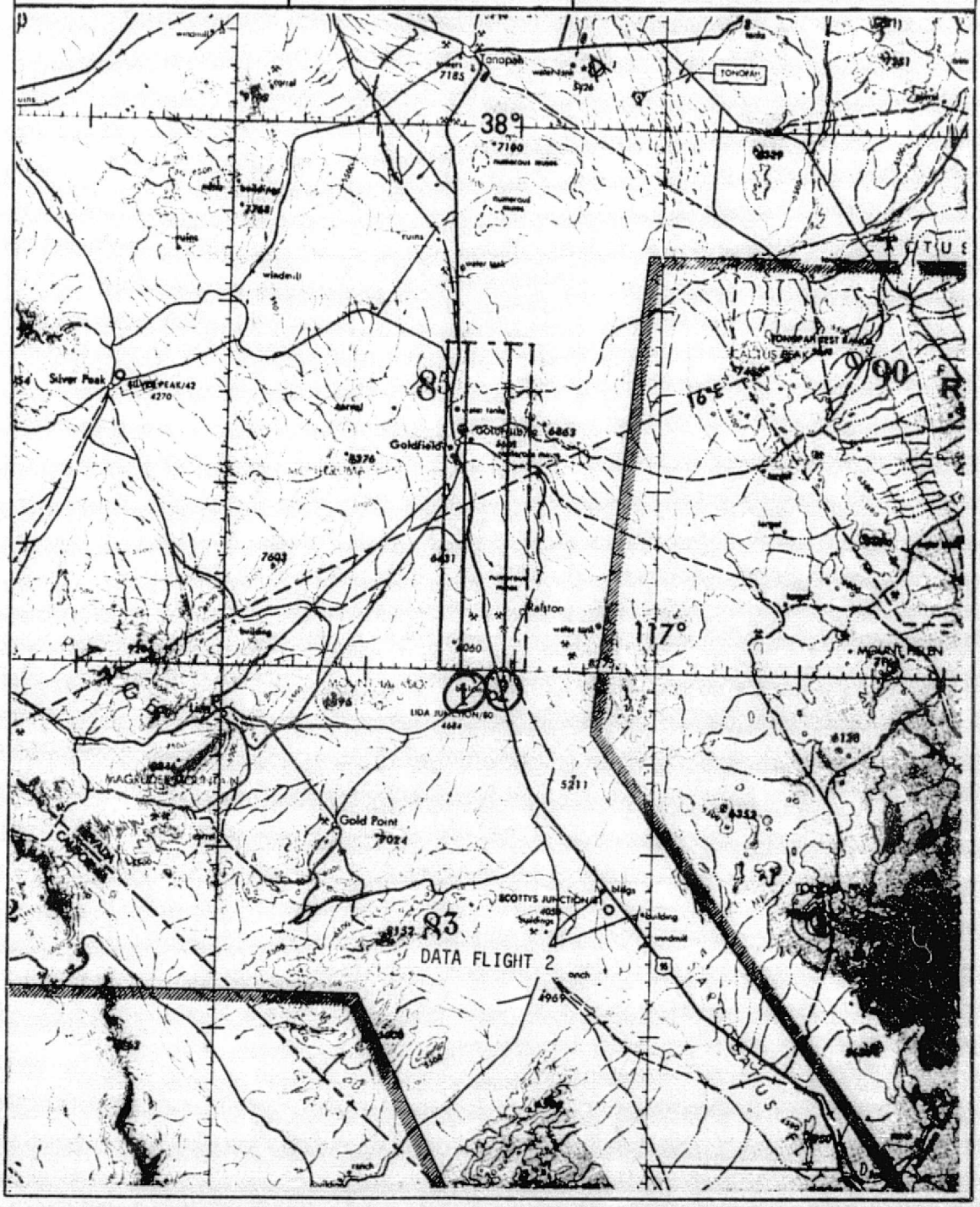

Figure 2-3. Ralston-Cuprite-Goldfield Flight Line

SECTION III

DATA PROCESSING

Computer processing of the 24-channel data involved the following: (1) a logging procedure which generated a separate data set from the original compacted data tape for each channel requested by the analyst; (2) characterization and removal of noise; (3) removal of geometric distortions; (4) degradation of resolution to that of LFO data; and (5) enhancement of the data through image processing techniques.

The data for each flight line was contained on up to eight individual data tapes. Each tape was logged and photo products were made for all the channels to be used in the analysis. This procedure enabled the analyst to determine which data tapes covered the area of interest as well as the general quality of the data contained in each of the requested channels. For example, in the Red Mountain area, there were two flight lines of three tapes each. The logging procedure showed that only two of the tapes for each flight line would be needed to cover the area of interest for this study and, of the nine channels requested, one of them was blank (no data was present). Further, of the remaining eight channels, at least six of them possessed a coherent horizontal banding in the data.

Most of the data had associated with it some type of noise. As mentioned above, the Red Mountain area data possessed coherent horizontal banding. The Goldfield, Ralston, and Tintic areas possessed random horizontal striping. To deal with the coherent banding problem, the following procedure was implemented: (1) the picture was rotated 90 deg so that the bands then appeared as columns; (2) the Fourier transform of each line (row) was computed; (3) the frequency component amplitudes were displayed, whereupon the coherent bands were represented by spikes; (4) these amplitudes were modified by notching out the offending frequencies, that is, by forcing these particular amplitudes to zero; (5) the inverse Fourier transform was made for each line, transforming the data back into picture form; (6) the picture was then rotated back to its original orientation.

Figure 3-1 gives an example of this procedure as applied to channel 5 of the Red Mountain study area. The method worked reasonably well although the procedure itself was quite time-consuming. The horizontal striping type of noise was random throughout the picture, hence treatment of this problem could not employ transform techniques. Instead, the following filtering procedure was used:

(1) The average of each line was computed and retained as a one-column "picture" ≡ PA.

(2) This picture was then low-pass-filtered with a 101 equal weight filter to yield the one column "picture" ≡ PAF. This size of filter was used to insure that all striping as viewed from the sample input picture would be smoothed out.

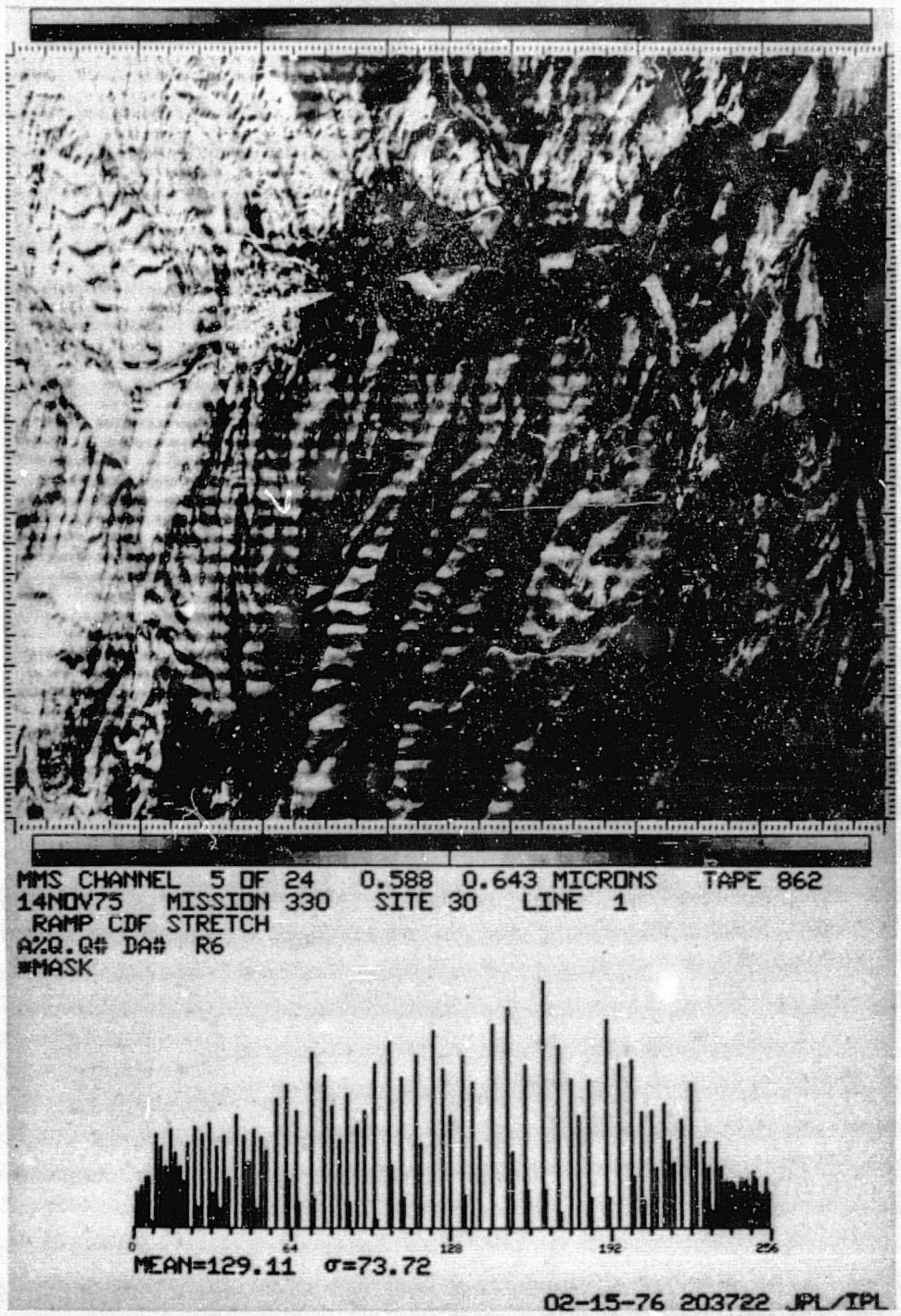

Figure 3-1. Red Mountain Test Site: Removal of Coherent Horizontal Banding

(a) Original Image

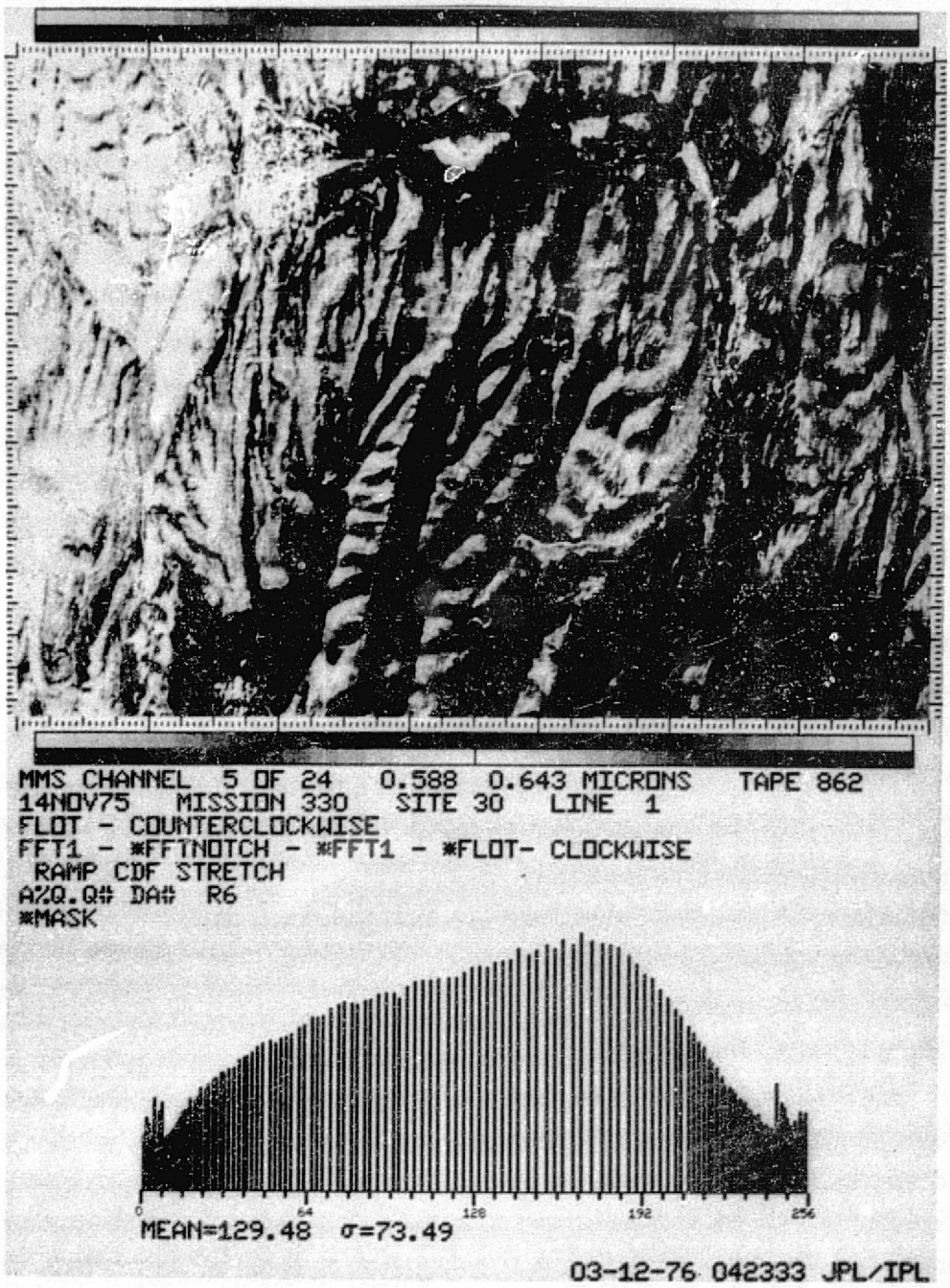

Figure 3-1. Red Mountain Test Site: Removal of Coherent Horizontal Banding

(b) After Noise Removal; Note That Only the Bottom 512 Lines of the Original Image Were Used

(3) The one-column difference picture (PA-PAF) was calculated, and then expanded to the full picture dimensions. That is, a picture with the same number of columns as the original was created, with each of its columns being identical with (PA-PAF).

(4) The above picture was then subtracted from the original to produce the end result.

Figure 3-2 illustrates this procedure as applied to channel 9 of an area just to the north of the Goldfield study area. This method was quite effective and was used extensively in reducing the noise in ratio pictures that were produced from the data.

The next step in processing was to remove geometric distortions introduced by the acquisition system. First, the data as received was inverted left to right so that it needed to be horizontally flipped. Second, a panoramic correction was made to account for the variation in ground area covered per data sample along a scan line. Third, the vertical:horizontal ratio (aspect ratio) was adjusted so that a data sample represented approximately a square area on the ground. For the Red Mountain area, the adjustment was a factor of 0.63 while for the Goldfield and Ralston areas the adjustment was a factor of 0.82. Both the aspect ratio and panorama corrections were performed by horizontal resampling of the data using linear interpolation. Finally, a geometric correction was made to compensate for deviations from a straight flight path and variations in aircraft orientation down the flight line. This correction was accomplished by the following procedure:

(1) Points that could be identified in a USGS topographic map were chosen from a picture representing the data. These points - called tiepoints - were referenced by line-sample coordinates in the picture and by the Universal Transverse Mercator grid system on the map. Due to lack of detail on the picture and/or the topographic base map, these tiepoints could only be chosen from certain areas within the picture.

(2) Using these known points, a second-order polynomial was fitted to the transformation from picture coordinates to map coordinates and a regular grid of tiepoints for the entire picture could be generated. This regular grid defined quadrilateral cells within the data set.

(3) A new picture was formed with the same geometry as the base map, whereupon within each cell, two-dimensional sampling using bilinear interpolation was performed to generate the new picture elements.

Figure 3-3 illustrates the application of all four of the above geometric corrections to channel 3 of the Goldfield study area.

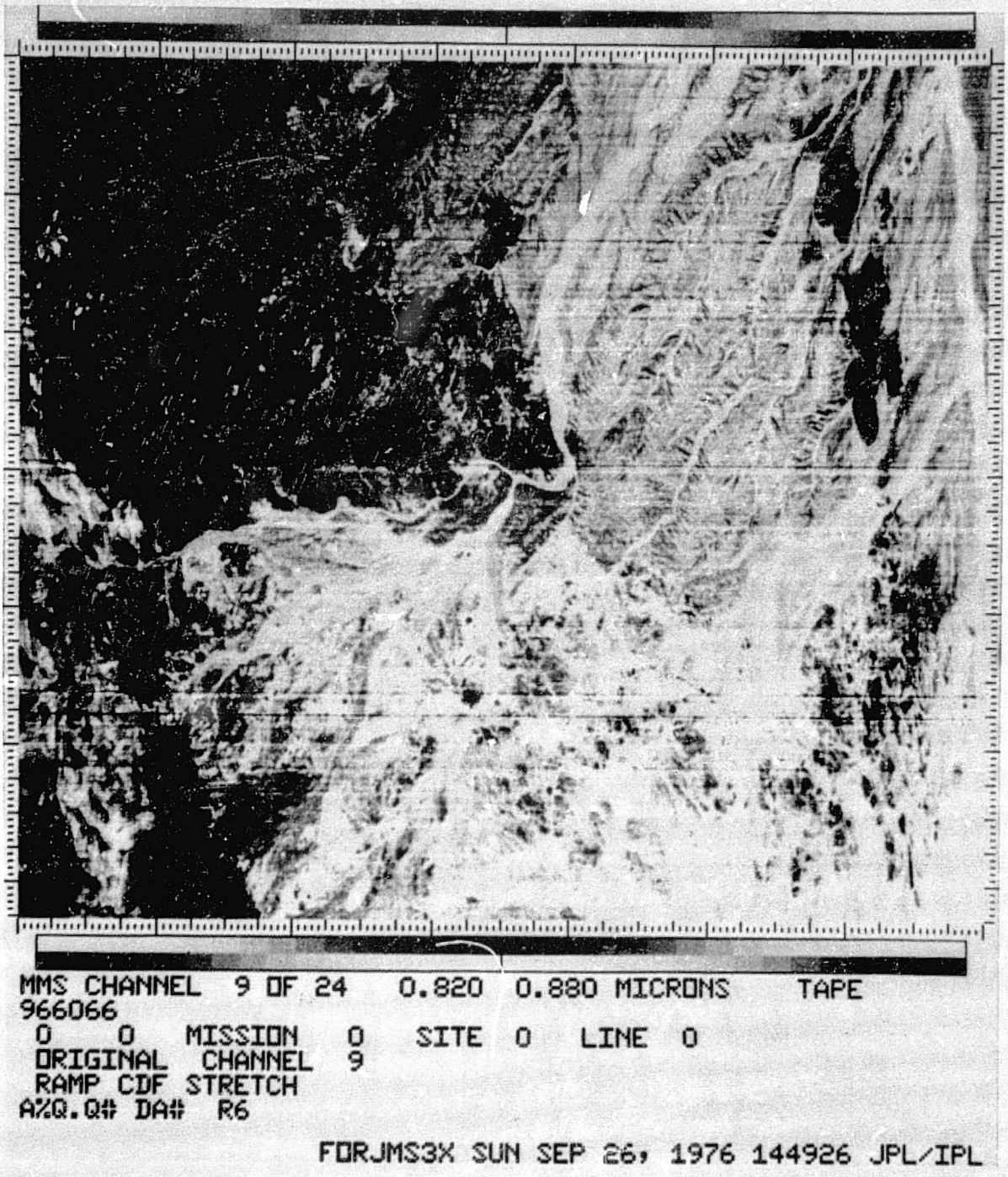

Figure 3-2. Goldfield Test Site: Removal of Random Horizontal Banding

(a) Original Image

ORIGINAL PAGE IS
OF POOR QUALITY

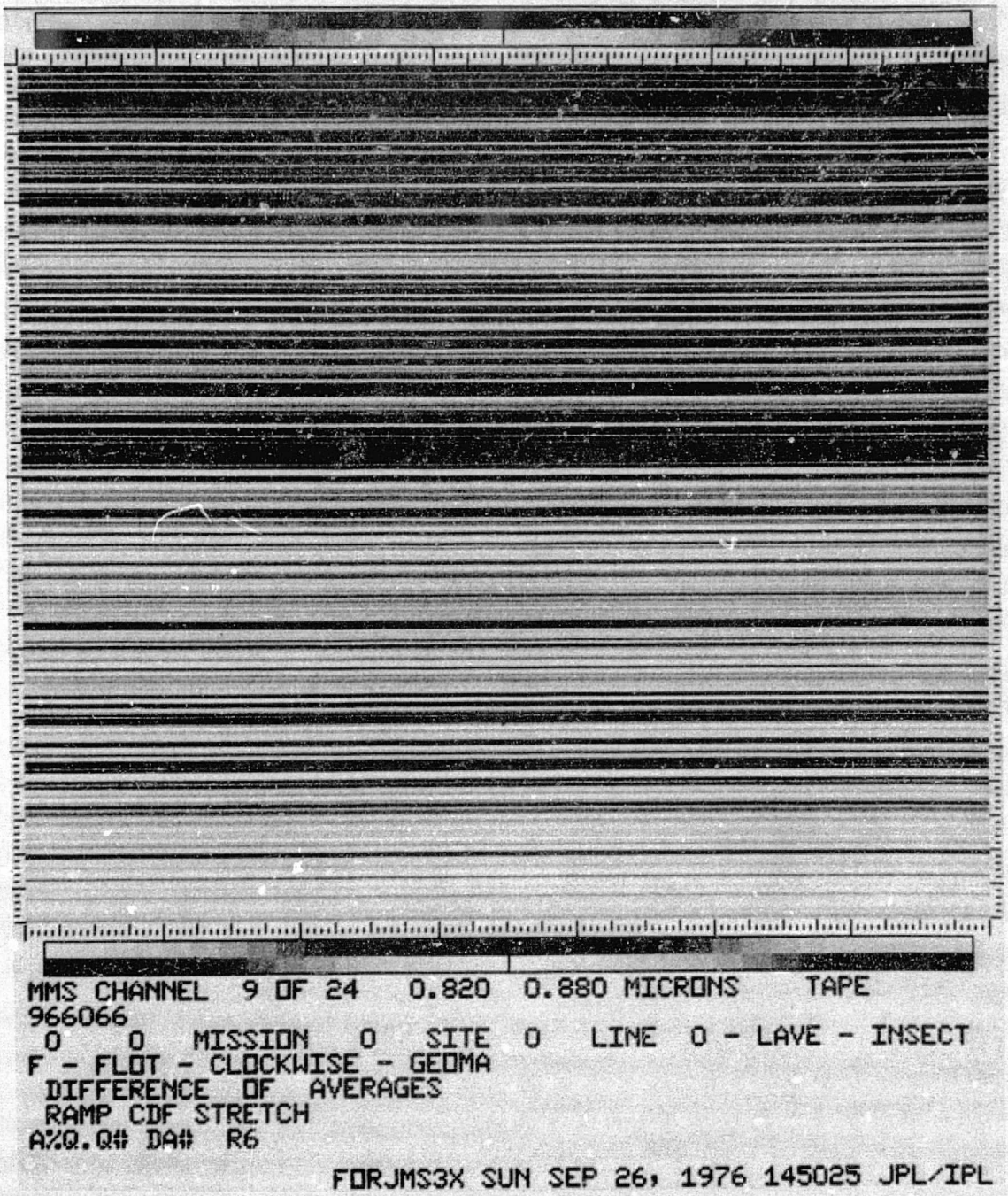

Figure 3-2. Goldfield Test Site: Removal of Random Horizontal Banding

(b) Expansion of the One-Column Difference Picture (PA-PAF) to Field Image Dimensions; This Image Has Been Contrast-Enhanced for Display Purposes.

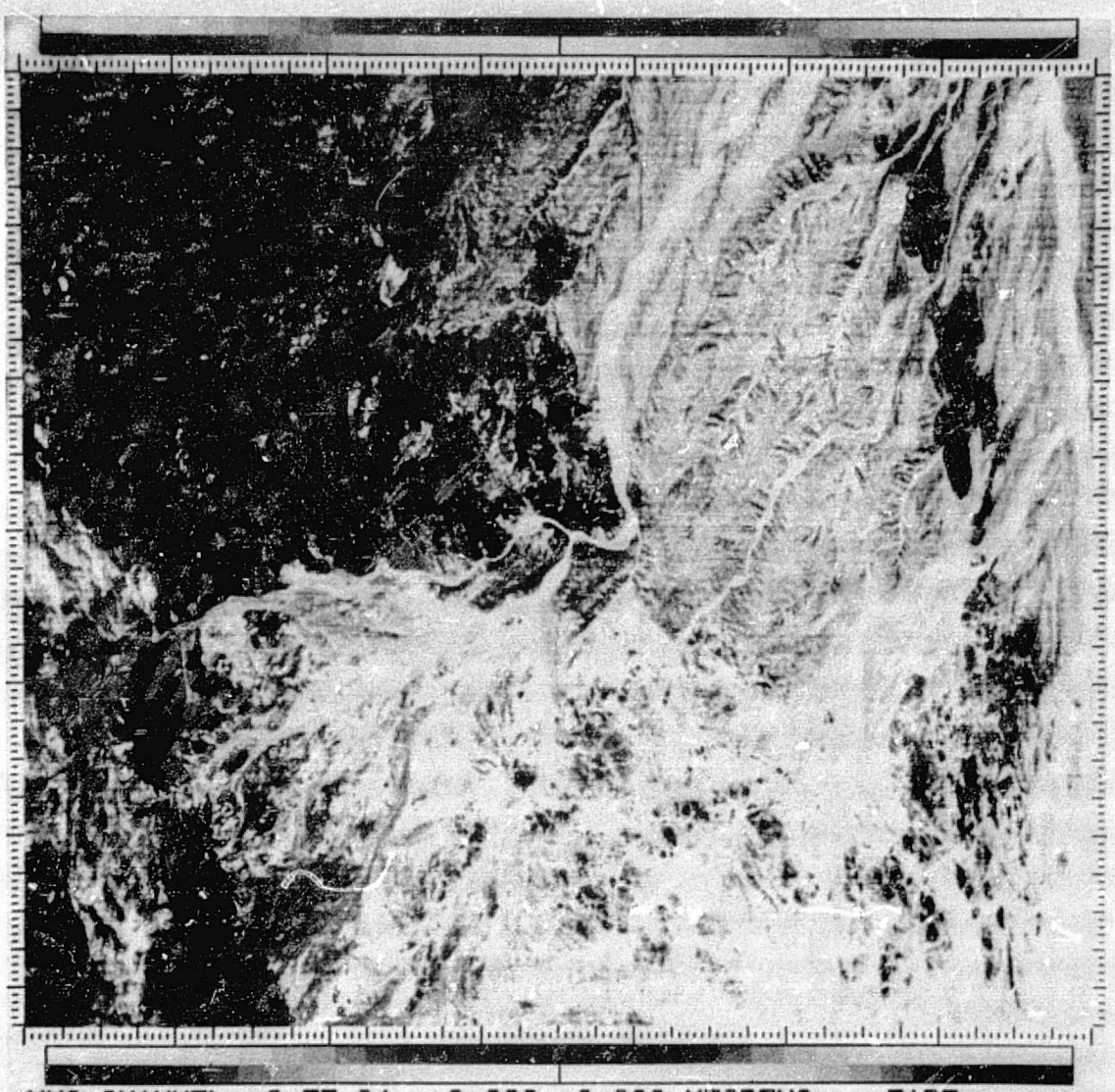

Figure 3-2. Goldfield Test Site: Removal of Random Horizontal Banding

(c) After Noise Removal

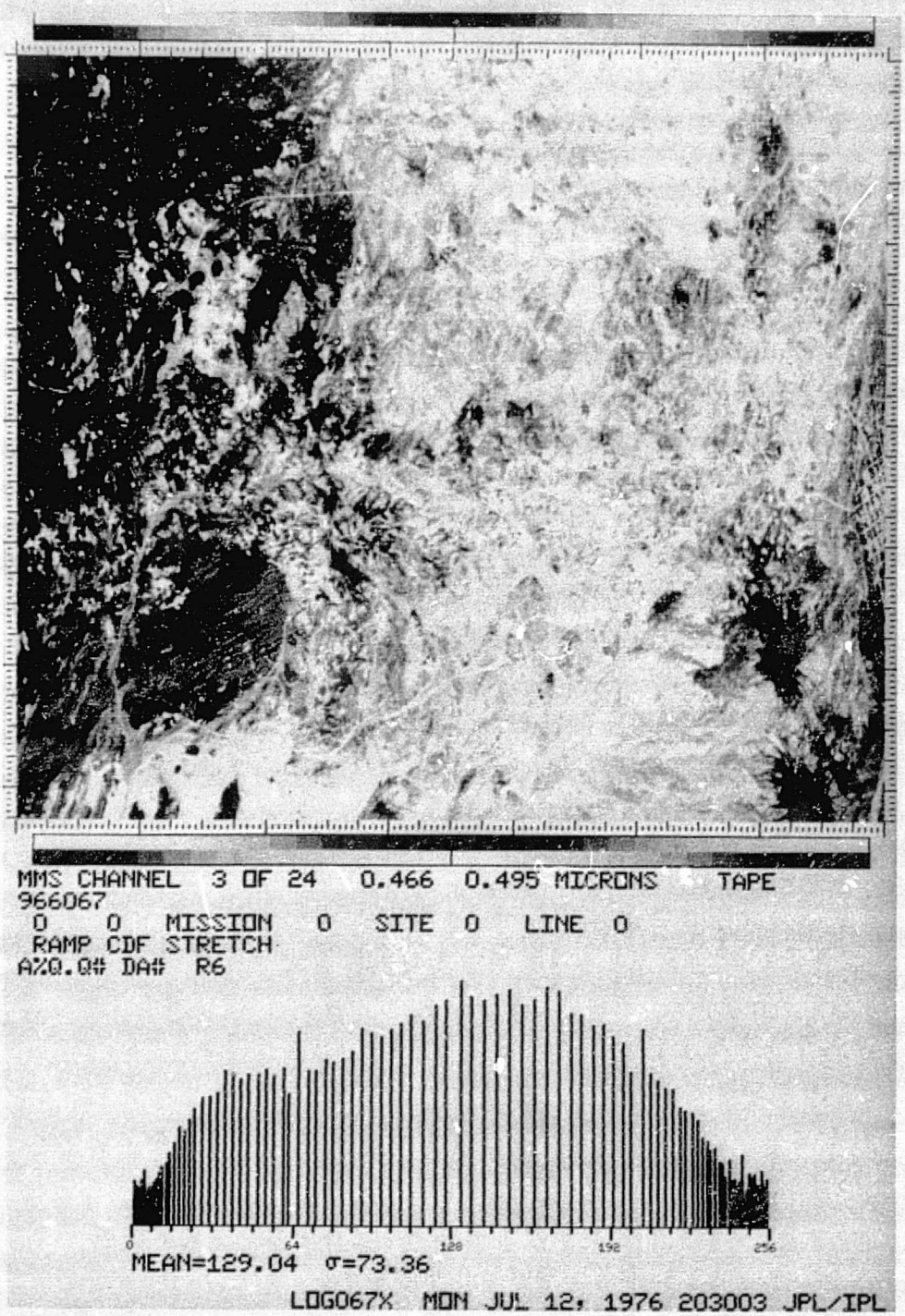

Figure 3-3. Goldfield Test Site: Removal of Geometric Distortions

(a) Original Image

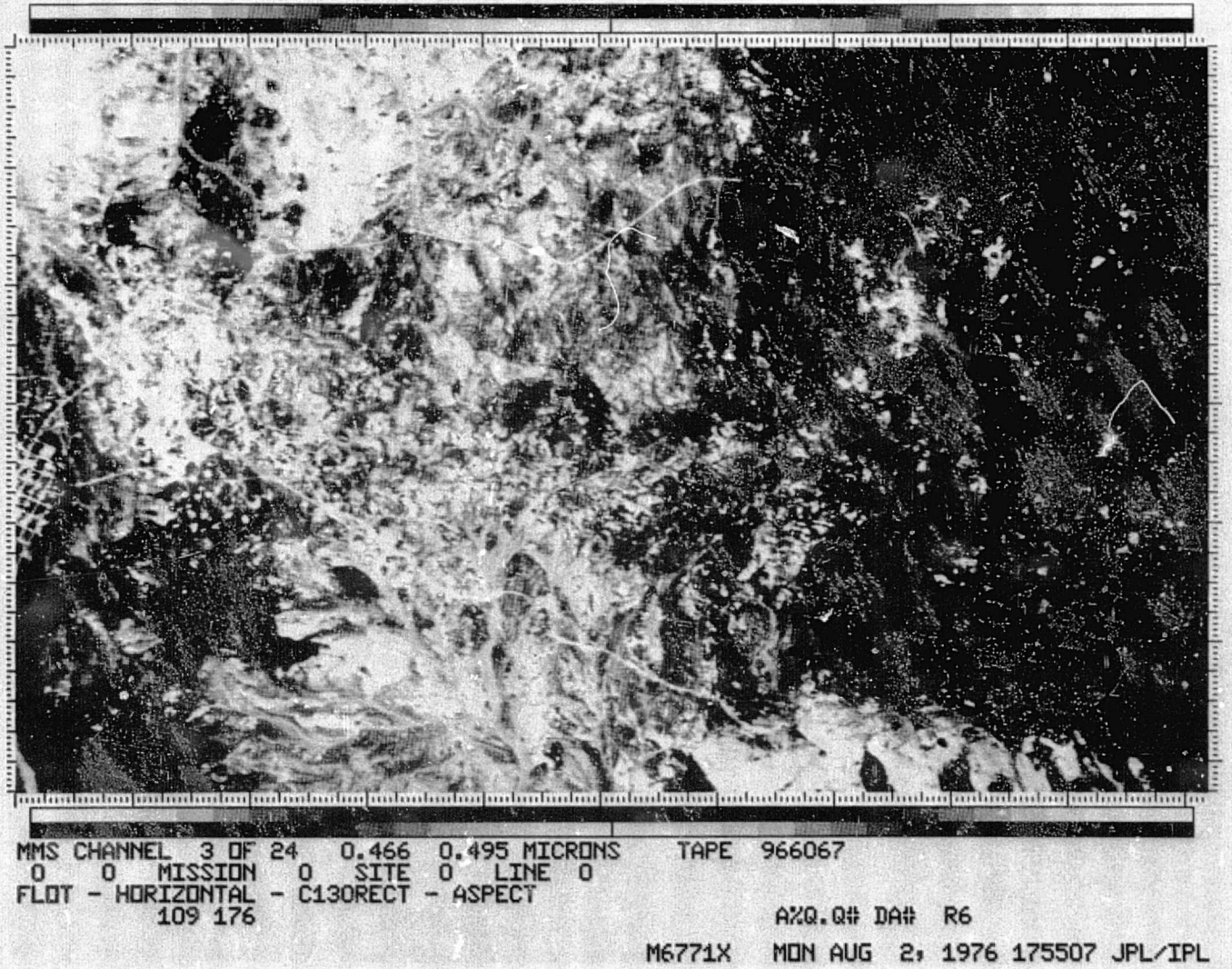

Figure 3-3. Goldfield Test Site: Removal of Geometric Distortions

(b) Image After Left-Right Inversion, Panorama Correction, and Aspect Ratio Correction

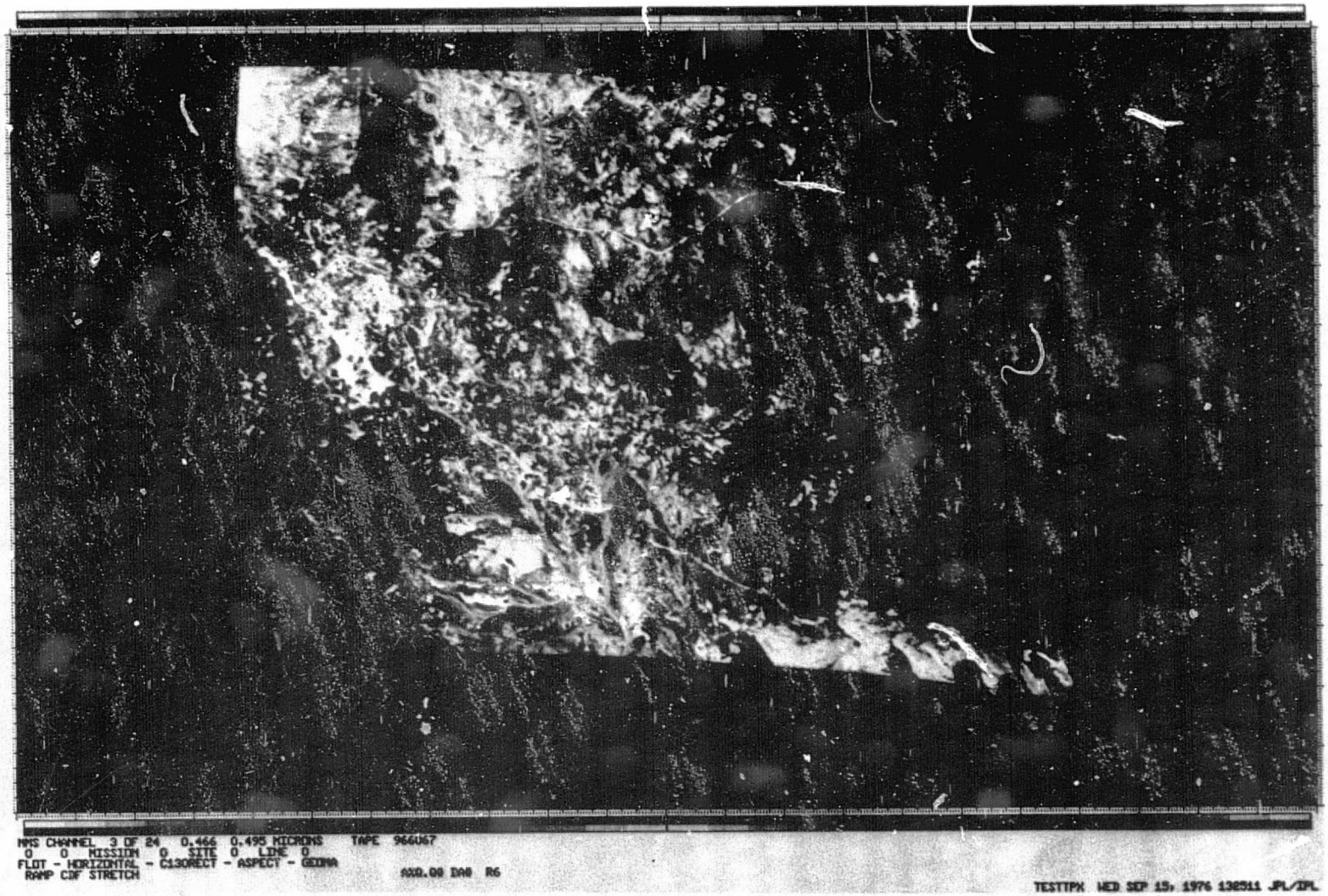

Figure 3-3. Goldfield Test Site: Removal of Geometric Distortions

(c) Final Result After Correction to Conform to the UTM Grid System of 7-1/2 foot Topographic Quadrangle Map

To directly compare the 24-channel data with the Landsat data, the resolution of the 24-channel data had to be degraded. For example, in the Goldfield and Ralston study areas, the data was first low-pass-filtered using a 5 x 5 box filter with unequal weights. These weights were chosen to produce a picture with 3.7 times less resolution.

Because we were unable to determine the frequency response characteristics of the Bendix scanner, no attempt was made to simulate the MTF (modulation transfer function) of the Landsat Follow-On sensors. While the spatial resolution degradation has the effect of increasing apparent MTF, the several geometric corrections which were applied tend to reduce high-frequency response, so, on balance, the effective MTF in the simulated pictures is probably reasonable. Similarly, since we did not know the sensitivity of the Bendix scanner, we did not adjust the intensity resolution of the images. Also, no increases to the signal-to-noise ratio were made, because noise levels were already high.

Since band ratios were to be the primary output product, brightness variations due to a range of viewing angles were not removed. This effect, usually described by a multiplicative photometric function, is removed by band ratioing.

In order to gain the most information from the data, each channel was contrast-enhanced (stretched) before a picture representing the scene was created. In all the study areas (Red Mountain, Goldfield, Tintic, Ralston) the histogram was made to approximate a uniform distribution. This enhancement has the property of providing a high degree of contrast which can then afford good discrimination of different features in the data. Ratio pictures were created using selected channels. The ratio program utilized computes an automatic gain and offset so that the output histogram occupies the entire dynamic range with a saturation of 0.5% at either extreme. A stretch was then applied to further increase the contrast of the ratio pictures.

SECTION IV

RED MOUNTAIN TEST AREA

The Red Mountain study area is located in southern Arizona near the town of Patagonia (Figure 2-1). Red Mountain is a 3 x 4 km mountain which consists of hydrothermally altered Tertiary volcanic rocks, and overlies a large unmined porphyry copper deposit. Tertiary alluvial fans, derived from Red Mountain, extend 2.5 km to the north. Other lithologies exposed locally include Tertiary extrusive and intrusive rocks of andesitic, rhyolitic and tuffaceous composition, and Quaternary surficial deposits. The volcanic and intrusive rocks at Red Mountain appear to be localized within a caldera type of subsidence structure that is bounded by faults and extensive zones of silicic intrusive breccias (Corn, 1975, Ref. 4-1). The dominant surface alteration on Red Mountain is pyritic argillic with the pyrite pervasively oxidized to limonite and geothite.

Figure 4-1 shows spectral reflectance measurements within the region of 0.4 to 2.4 μm, acquired with JPL's Portable Field Reflectance Spectrometer (Goetz, et al., 1975, Ref. 4-2) for representative altered areas on Red Mountain. The solid curve is the spectrum of a strongly silicified, non-limonitic altered area. The broken curve is from an altered area with heavy limonite and hematite occurrences. The broad absorption band centered at about 0.85 m is due to the electronic transition of ferric iron, Fe^{3+}; the absorption band at 2.2 μm is due to vibrational overtones of OH associated with hydrous minerals (such as clays). The silicified material shows the same absorption at 2.2 μm, lacks the Fe^{3+} absorption band and has a steeper rise in reflectivity from 1.3 to 1.6 μm than the limonitic material. Landsat 1 and 2 MSS data are restricted to the wavelength region of 0.5 to 1.1 μm. Therefore, any computer processing of the data is done to take advantage of and to display the anomalous Fe^{3+} absorption band at 0.85 μm.

Landsat 1 MSS data (1678-17210, June 1, 1974) were computer processed and analyzed for detection of the alteration areas. A false color ratio composite was produced by using ratios 4/5, 5/6, and 6/7 (Rowan, et al., 1972, Ref. 4-3), displayed as blue, green, and red respectively for color reconstruction (Figure 4-2). Ratioing removes, to the first order, brightness effects due to topography, exaggerates subtle color differences, and gives a better representation of a material's spectral characteristics.

Red color anomalies on the image were observed on the flanks of Red Mountain, coinciding with the northward-shed alluvial fans and with limonitic alteration on the south and west. Several small red areas east of Red Mountain also show limonitic alteration. The red color reflects a relatively large value of the 6/7 ratio (.7 - .8μm/.8 - 1.1μm). This ratio is larger for materials having an Fe^{3+} absorption band than for materials lacking this band (Figure 4-1). The bright circular area in the center of the image corresponds to outcrops of dark purple andesite. The spectral reflectance curve for this material

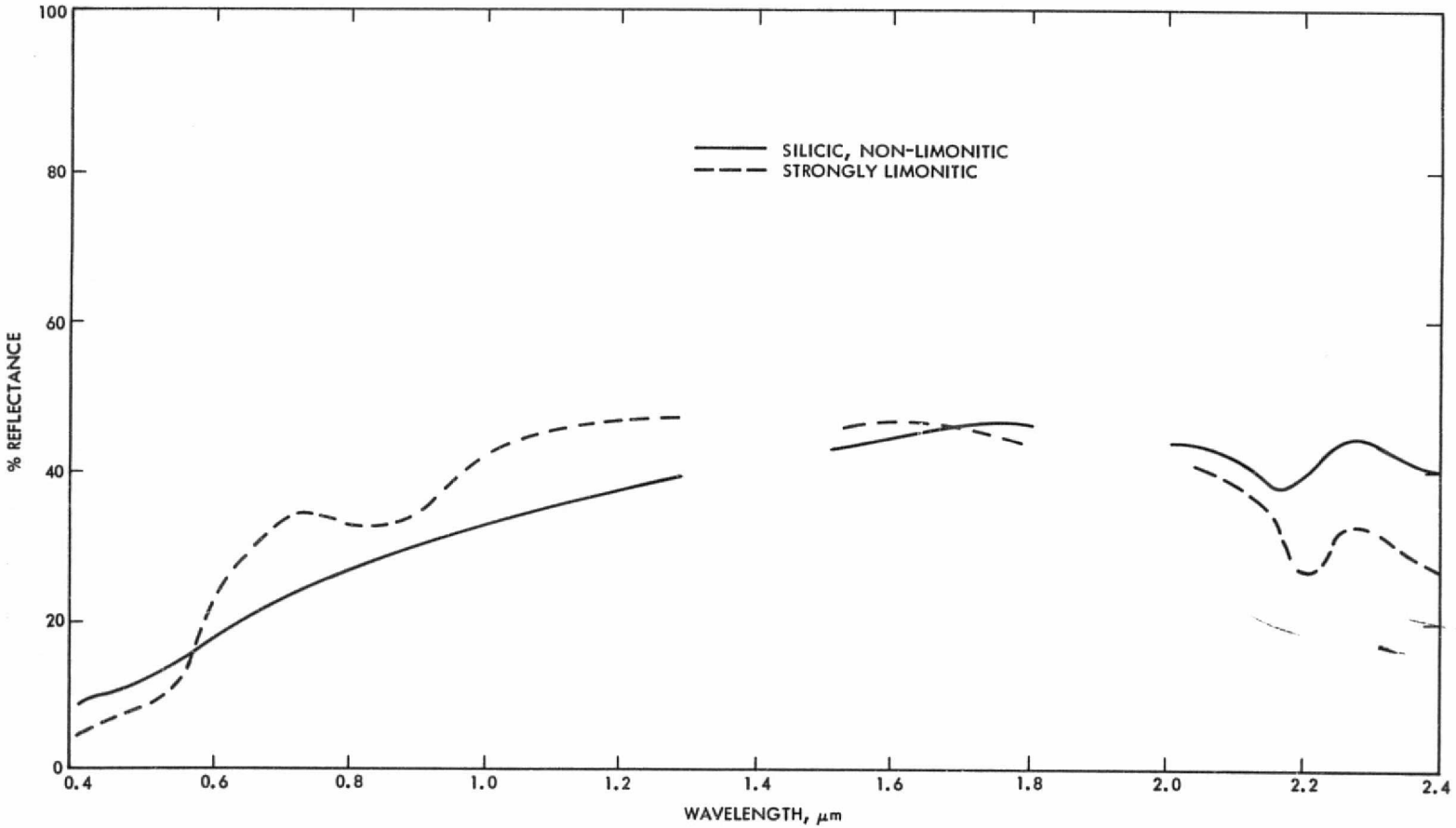

Figure 4-1. Spectral Reflectance Curves of Altered Material at Red Mountain; Curves Normalized to Fiberfrax Standard

Figure 4-2. Red Mountain Test Area: Landsat False-Color Ratio Composite; Band-to-Band Ratios 4/5, 5/6, 6/7, Displayed as Blue, Green, and Red, Respectively.

is relatively flat, so that the values for the three ratios 4/5, 5/6, 6/7 are relatively large, resulting in a color contribution from each ratio which produces a white color in the ratio composite. Areas of heavy vegetation are blue (along Sonoita Creek and on Red Mountain). No silicic zones are identifiable.

To examine the separability of altered rocks with LFO bands, simulated wavelength bands were used to create several color composite pictures: (1) "true" color, (2) false color infrared, and (3) color ratio composite.

The "true" color image was produced by standard color reconstruction techniques, displaying MSDS channels 3, 4, and 6 with blue, green, and red light, respectively. Analysis of the resulting color image indicated that no areas of hydrothermal alteration could be detected. Red Mountain was green-brown in color, and vegetated areas were green. Regions of known alteration were not distinctly colored, with the exception of a few small areas of intense bleaching, which appeared white.

The false color infrared composite was produced by projecting MSDS channels 4, 6, and 9 with blue, green, and red light, respectively. This combination is similar to the standard Landsat false color infrared composite (MSS bands 4, 5, and 7). A comparison with the Landsat color pictures indicated that the LFO simulated picture was generally similar. Red Mountain appeared red, the northward-shed alluvial fan was red-yellow in color, the area east of Red Mountain was red where vegetation was present and blue-green where there was little vegetation; no alteration zones were identifiable. This is consistent with previous work in Nevada with Landsat data which showed that alteration zones were very difficult to identify using a false color infrared composite (Rowan et al., 1974, Ref. 4-3).

A color ratio composite, using simulated LFO data, is shown in Figure 4-3. Displayed as blue, green, and red are ratios 1.52 - 1.73/.82 - .87 μm, 1.52 - 1.73 μm/.46 - .50 μm, and .64 - .68 μm/.46 - .50 μm, respectively.

Based on a previous statistical analysis of spectral reflectance data (Goetz, et al., 1975a, Ref. 4-4), the optimal wavelength regions for discriminating between altered and unaltered volcanic rocks were 2.2, 1.6, and 1.3 μm. Of these, only the 1.6 μm region coincides with a proposed LFO spectral band. The other ratios were chosen to enhance the differences in slope of the spectral response of limonitic vs non-limonitic rocks, based on field spectral reflectance measurements.

Due to the heavy vegetation cover, Red Mountain appears green and yellow. Iron-rich alteration on Red Mountain appears red and orange in those areas which are less heavily vegetated and yellow in those areas with moderate vegetation. The northward-shed alluvial fan, composed of iron-rich altered debris, appears reddish on the imagery. Areas of bleached silicic alteration appear blue on Red Mountain. They are mainly confined to ridge tops, as the silicic zones are very resistant. To the east of Red Mountain the blue areas are also made up of highly silicic, bleached rocks with minor occurrence of iron-rich

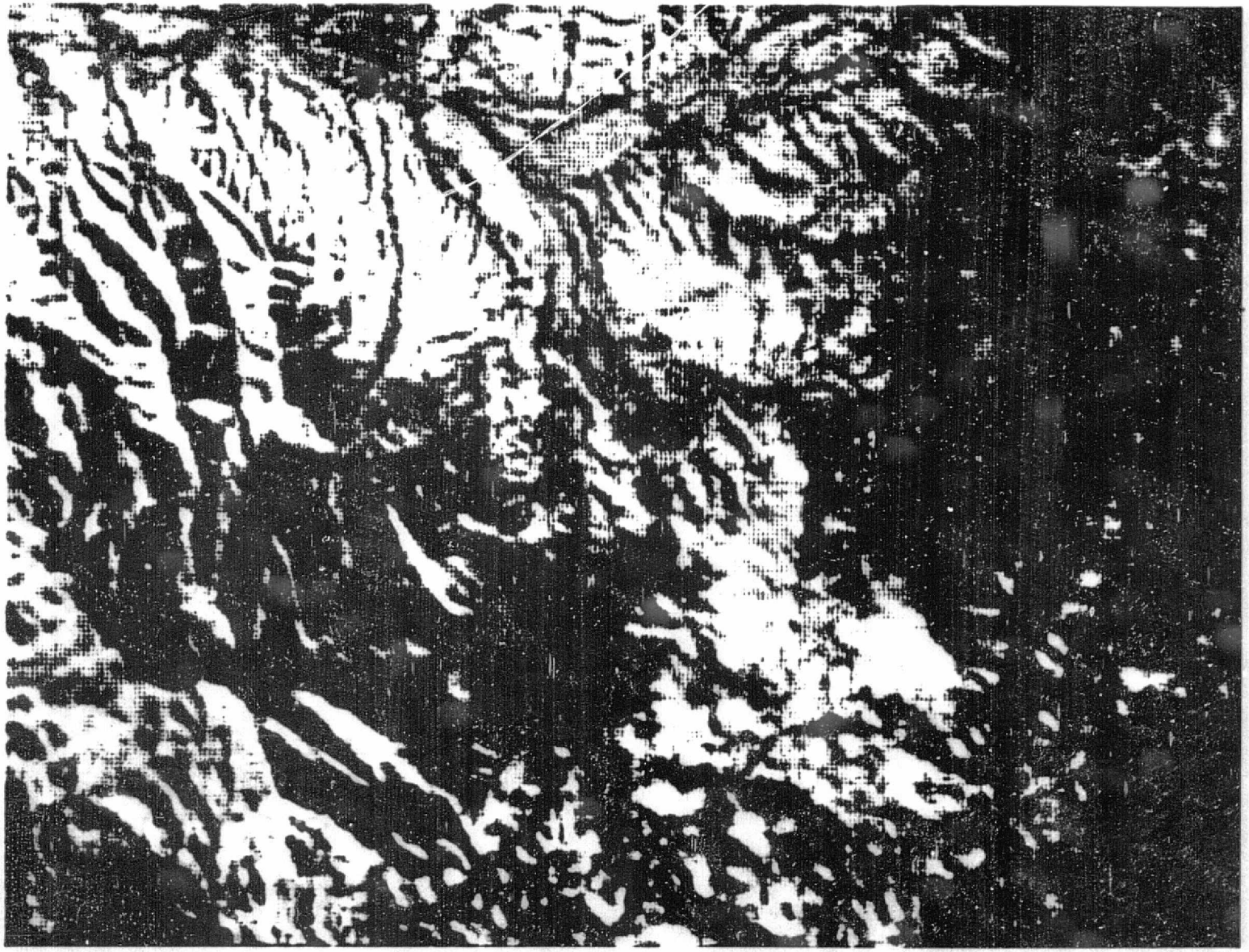

Figure 4-3. Red Mountain Test Area: False-Color Ratio Composite Using Simulated LFO Bands; Ratios 1.6/.85μm, 1.6/.48μm, .66/.48μm Displayed as Blue, Green, and Red, Respectively

alteration. The maroon area adjacent to Red Mountain on the east side is a region of outcrop of dark purple andesite. On the north side of Red Mountain, a blue to purple linear feature is a porphyry dike that has been strongly silicified (blue) with some iron remaining (red), hence the purple color. All the altered areas are fairly distinct in color with respect to both the heavily vegetated areas and the different kinds of alteration.

One area of ambiguity is an uncultivated field in the north-central part of the image, which appears blue on the color composite. Laboratory spectral reflectance measurements (Figure 4-4) of the soil indicate that the soil has the same ratio values as silicified rocks in the Landsat-D bands. The addition of a band at 2.2 μm would eliminate this ambiguity by distinguishing between materials with hydrous minerals (altered rocks) and those lacking hydrous minerals.

The proposed LFO parameters (increased resolution and additional wavelength bands) substantially increase the ability to discriminate and separate altered materials at Red Mountain. The wider spectral coverage allows separation of non-limonitic altered materials from altered silicified materials. This separation cannot be made using Landsat 1 or 2 multispectral data, where only iron-rich altered materials can be identified.

The increased resolution (30 m versus 80 m for Landsat 1 and 2) allows identification of features too small to be seen on Landsat 1 and 2 imagery. Analysis of the LFO simulation imagery for Red Mountain allows identification of (1) small silicified knobs on Red Mountain, (2) the altered porphyritic dike on the north side of Red Mountain, and (3) small, iron-rich alteration patches in the area.

Preliminary analysis of the MSDS data was published as a JPL Technical Memorandum and is included as Appendix A.

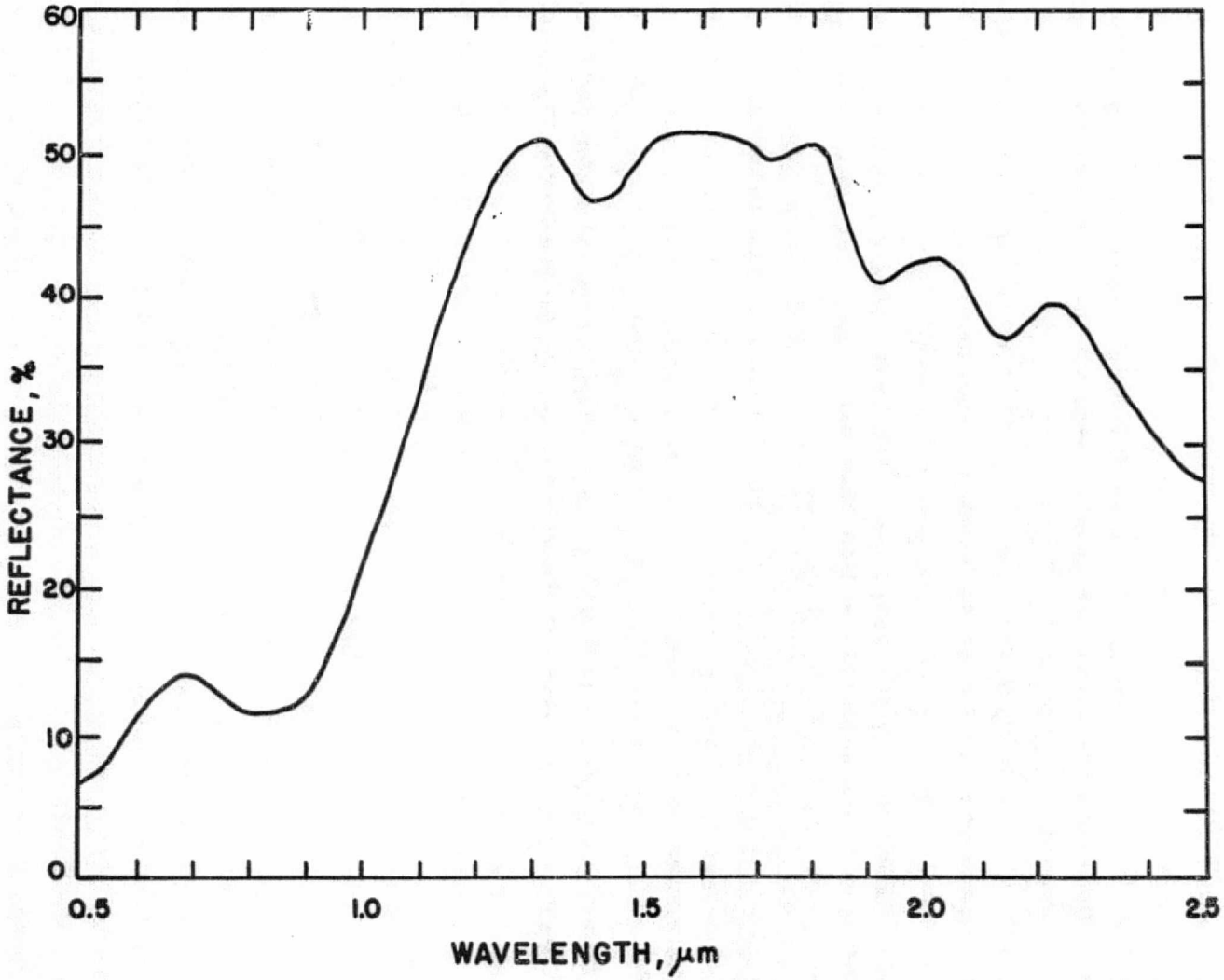

Figure 4-4. Spectral Reflectance Curve of Soil Sample from Red Mountain Test Area

SECTION V

CUPRITE-RALSTON TEST AREA

The Cuprite-Ralston test area is located at the southern end of the Goldfield flight line. The district is located 35 km south of the town of Goldfield, in south central Nevada (Fig. 2-1). The district includes exposures of hydrothermally altered rocks totaling about 12 km, and occurs in two areas separated by U.S. Highway 95. Minor sulfur, silica, and possibly precious metal production is attributed to the hydrothermally altered parts of the district (Albers & Stewart, 1972, see Appendix B).

The area chosen for study was the eastern of the two altered areas. Here alteration affects volcanic and sedimentary rocks of Tertiary age. Altered rocks form three mapable zones: argillized rocks, opalized rocks (opalites), and silicified rocks. Silicified rocks are the most intensely altered and argillized rocks are the least altered.

A color ratio composite using Landsat band ratios 4/5, 5/6, and 6/7 (Rowan et al., 1974, Ref. 4-3) was produced. This combination displays variations in the intensity of ferric-iron absorption bands and is effective for mapping limonitic altered rocks. In the Cuprite-Ralston area, only argillized rocks and limonitic opalites could be detected; none of the bleached silicified rocks were identifiable. Analysis of 0.45 - 2.45-μm field reflectance spectra showed that the iron-deficient opalites have an intense OH^- absorption band near 2.2 μm owing to their clay mineral and alunite contents and that this feature is absent in adjacent unaltered tuffs and basalts.

To evaluate the usefulness of this spectral feature for discriminating between altered and unaltered rocks, we generated a color ratio composite image from MSDS multispectral data, using band ratios 1.6/2.2μm, 1.6/.4μm, and 0.6/1.μm (these are band centers). The altered rocks could be discriminated from unaltered rocks with few ambiguities. In addition some effects of mineralogical zoning could be discriminated and four altered rock types were distinguishable: bleached opalites, opalites with iron, silicified rocks, and argillized rocks. Appendix B contains a detailed description of the test site and presents the results of using the MSDS data for detection of alteration.

As part of the LFO simulation study, principal component analysis (Karhuenen-Loeve Transformation) was applied to the MSDS data. This technique is a dimension reduction algorithm which constructs orthogonal linear combinations of the input data; the first component contains the majority of the scene information, the second component less information, etc.

Figure 5-1 is a color reconstruction using this transformation on MSDS channels 3, 4, 5, 6, 8, 9, and 12 (which simulate the proposed LFO bands). The first component is displayed as blue, the second as green, and the third as red. Unaltered volcanic rocks are red in

Figure 5-1. Cuprite-Ralston Area: Principal Component Transformation Using MSDS Channels 3, 4, 5, 6, 8, 9, 12

the image, the playas white, argillized rocks are yellow, opalized rocks are light pink, and iron-bearing rocks are blue. The only altered materials that are not adequately separable are (1) the silicified rocks in the center of the area, and (2) opalites with varying amounts of iron. Nevertheless, this image allows much better separation of altered materials than the present Landsat data (see Appendix B).

The same principal component analysis was performed with the addition of MSDS bands 11 and 13 (1.3 and 2.2 μm) to the input variables (Figure 5-2). All of the altered materials are separable, though to a lesser degree than using spectral band ratios (Appendix B). These images indicate that information from the 1.3- and 2.2-μm wavelength regions is critical for separation of altered volcanic rocks.

From the present analysis we conclude that intelligent choice of band ratios produces a better display for interpretation than use of principal component analysis, which is in essence an unsupervised classifier. A priori knowledge of the spectral behavior of the materials of interest allows selection of the spectral bands whose ratios can maximize the differences between particular rock types. Principal component analysis, on the other hand, deals with the differences of all the materials in a scene, not necessarily those of primary importance.

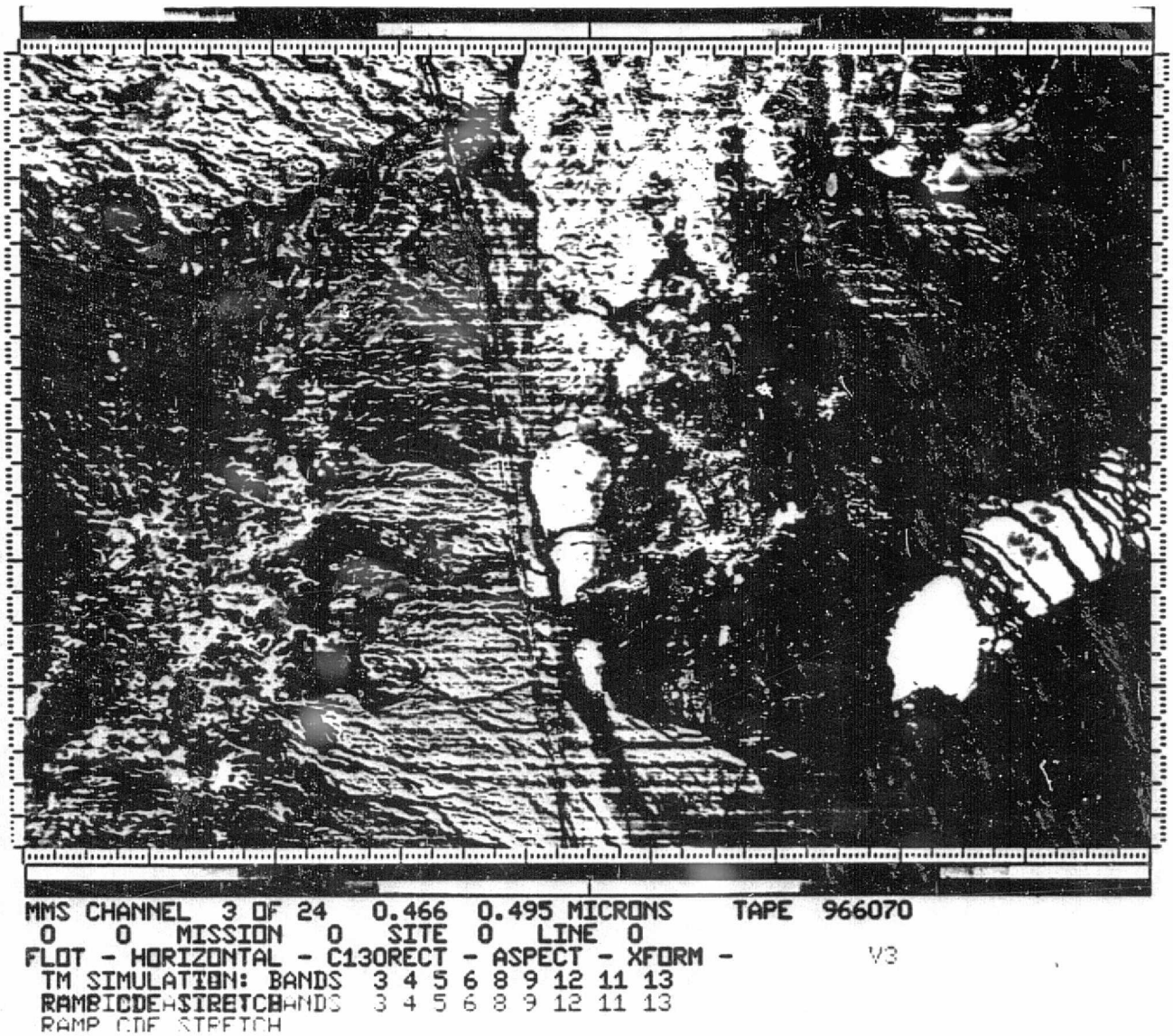

Figure 5-2. Cuprite-Ralston Area: Principal Component Transformation Using MSDS Channels 3, 4, 5, 6, 8, 9, 12, 11, 13

SECTION VI

CONCLUSIONS

1. Landsat MSS data can only be used to discriminate hydrothermally altered rocks which contain associated iron oxide minerals.

2. Using multispectral data from the first five LFO proposed wavelength bands, additional alteration types can be detected. At the Red Mountain test site, it was possible to identify silicified areas. At the Cuprite-Ralston test site opalized rocks and argillized rocks could be discriminated.

3. The addition of a spectral band at 2.2 μm allows even better discrimination of hydrothermal alteration types. This was demonstrated for the Cuprite-Ralston test site, where four types of alteration could be discriminated.

4. The increased resolution of LFO allows discrimination of smaller features than Landsat MSS allows. At Red Mountain it was possible to identify a silicified, iron-rich dike that could not be seen on Landsat. Small silicic knobs could also be recognized.

5. Use of band ratioing proved more effective than principal component transformations for discrimination of alteration types. This is due to the ability of the investigator to choose bands for ratioing which he knows to contain spectral features associated with alteration; principal component transformation is an unsupervised classifier, nonspecific for any particular material in a scene.

REFERENCES

2-1. NASA Earth Resources Program, JSC Earth Resources Program Plan, Lyndon B. Johnson Space Center, Houston, Texas, November 1975.

4-1. Corn, R.M., 1975, "Alteration - Mineralization Zoning, Red Mountain, Arizona," Economic Geology, Vol. 70, pp. 1437-47.

4-2. Goetz, A. F. H., Billingsley, F., Gillespie, A., Abrams, M., Squires, R., Shoemaker, E., Luchitta, I., Elston, D.P., 1975, "Application of ERTS Images and Image Processing to Regional Geologic Problems and Geologic Mapping in Northern Arizona," JPL TR32-1597, NASA-Jet Propulsion Laboratory, Pasadena, California.

4-3. Rowan, L., Wetlaufer, P., Goetz, A., Billingsley, F., Stewart, J., 1974, "Discrimination of Rock Types and Altered Areas in Nevada by the Use of ERTS Images," U.S. Geological Survey Professional Paper 883, Washington, D.C.

4-4. Goetz, A.F.A., Siegal, B.S. Rowan, L.C., 1975, "Quantitative Spectral Techniques and Computer Image Processing as Applied to Lithologic Mapping," Proc. of 1975 IEEE Conference on Decision and Control, pp. 412-413, Houston, Texas, December 10-12, 1975.

APPENDIX A

DETECTION OF ALTERATION ASSOCIATED WITH A PORPHYRY COPPER DEPOSIT IN SOUTHERN ARIZONA

ABSTRACT

The author has identified the following significant results. Alteration associated with a known porphyry copper deposit, Red Mountain near Patagonia, Arizona, has been delineated using spectral reflectance data, acquired by Landsat, a field spectrometer, and by NASA's Bendix 24-channel Multispectral Scanner (MSDS).

Computer processing of Landsat MSS data was performed using contrast stretching and band-to-band ratioing. A false color ratio composite picture showed color anomalies which coincided with known areas of alteration on and about Red Mountain. A helicopter survey of the study area was undertaken using the Jet Propulsion Laboratory's portable field reflectance spectrometer. One hundred and fifty-six spectra were obtained in the 0.4 to 2.5 μm wavelength region. The spectra were digitized and contour maps for 24 wavelength intervals were produced; no spectral anomalies were evident for the known altered areas. A contour map produced from the 1.6 and 2.2 μm ratio generally delineated the alteration areas. The 1.3, 1.6, and 2.2 μm wavelength data were canonically transformed using a transformation empirically derived from discriminant function analysis of altered and unaltered materials for the Goldfield, Nevada region, and a contour map was produced for the first canonical variable. The known areas of alteration were clearly defined on the contour map. Spectral reflectance imagery in the 0.4 to 2.5 μm wavelength region was obtained with NASA's Bendix 24-channel MSDS. A false color ratio composite was created using the following ratios: 1.5/.82, 1.5/.46 and .65/.46, chosen to give the maximum differences between altered and unaltered rock. The alteration

areas in and around Red Mountain were identifiable. Good separation was observed between limonitic alteration centered on Red Mountain and alluvial fans shed northward, and areas of silicic, non-limonitic alteration to the east.

This paper presents the results of a joint Jet Propulsion Laboratory-Continental Oil Company-Kerr McGee Oil Company project to develop remote sensing exploration techniques for identifying hydrothermal alteration zones associated with porphyry copper deposits. The study area centers around Red Mountain in Southern Arizona, near the town of Patagonia. Red Mountain, a 3 x 4 km mountain, consists of hydrothermally altered Tertiary rhyolitic rocks, and overlies a large unmined porphyry copper deposit. Tertiary alluvial fans, derived from Red Mountain, extend 2.5 km to the north. Other lithologies exposed locally include Tertiary and Mesozic extrusives and intrusives, and Paleozoic sediments.

Three types of data were analyzed in an attempt to delineate the areas of hydrothermal alteration: 1) Landsat MSS imagery; 2) Helicopter-acquired reflectance spectra; and 3) MSS imagery acquired with NASA's Bendix 24-channel scanner. Computer processing algorithms, developed during a study of alteration at Goldfield, Nevada, were applied to the data.

Two sets of Landsat MSS computer tapes were acquired for the test area, E-1156-17280 (December 26, 1972) and E-1678-17210 (June 1, 1974). Preliminary computer processing of both sets of tapes was performed to remove noise, correct dropped data lines, and rectify geometric distortions resulting from the Earth's rotation and satellite motion. Pictures were produced from each set of tapes for the four MSS spectral bands. Examination of the December pictures indicated excessive seasonal vegetative cover and extreme shadowing due to low sun angle. These factors rendered the pictures unsatisfactory for further study.

Vegetative cover and shadowing were less on the June pictures. Band-to-band ratios were constructed from the digital data. (Ratio images remove, to the first order, variations in brightness due to topography, and thus gave a truer picture of the spectral characteristics of a material.) Three ratio positive transparencies (4/5, 5/6 and 6/7) were combined on an additive color viewer to produce a false-color composite picture. Ratio 4/5 was projected as blue, 5/6 as green, and 6/7 as red. A subtle but noticeable red color anomaly centered on Red Mountain was observed. Other less obvious red color anomalies observed in the vicinity of Red Mountain were: 1) an area adjacent to the northwest of Red Mountain, coinciding with the alluvial fans flanking Red Mountain; 2) an area about 8 km to the northwest; and 3) an area about 5 km east of Red Mountain. These three areas also correspond to areas of known hydrothermal alteration.

In order to obtain a better understanding of the spectral characteristics of the altered rocks at Red Mountain, a field reconnaissance of the test area was undertaken and samples were collected from three sites of known hydrothermal alteration. Laboratory measurements of the spectral reflectivity in the 0.5 to 2.5 μm wavelength region (see Figure 1) revealed prominent absorption bands at 0.85 μm, 1.4 μm, 1.75 μm, 1.9 μm, and 2.15 μm. The 0.85 μm absorption band is associated with ferric iron, a constituent of limonite, hematite, and goethite, which are minerals characteristic of alteration. Absorption bands at 1.4 μm and 1.9 μm are characteristic of adsorbed water of hydrous minerals such as limonite. The 1.75 μm and 2.15 μm absorptions are assigned to the OH^- stretching of clay minerals, which are also characteristic of hydrothermal alteration.

In the wavelength region spanned by the Landsat MSS, 0.5 μm to 1.1 μm, only the absorption band at 0.85 μm due to ferric iron can be detected. The influence of this absorption band is to strongly depress the reflectance of altered rocks in MSS bands 6 and 7, and is inferred to be the cause of the color anomaly seen in the false color ratio composite picture.

As part of a broader research program to determine the optimal wavelength regions for identifying hydrothermal alteration, an aerial survey of the test area was performed using the Jet Propulsion Laboratory's portable reflectance spectrometer. The spectrometer measures reflectivity in the range of 0.4 to 2.5 μm. Measurements were acquired by helicopter for a 9 x 10 km area about Red Mountain. One hundred fifty-six spectra, each covering a 9 x 25 m area, were obtained based on a rectilinear sampling grid with 80 m spacing. The spectra were digitized at 0.05 μm intervals for the wavelength region of 0.4 to 1.0 μm and 0.10 μm intervals thereafter. Contour maps were produced for each of the 24 intervals; no spectral anomalies were evident for the known alteration areas.

Based on previous analysis of spectra of hydrothermally altered and unaltered materials in Goldfield, Nevada, a contour map was produced from the ratio of the 1.6 μm and 2.2 μm wavelength region. High ratio values are indicative of hydrothermally altered materials. The highest ratio values on the contour map of Red Mountain delineated, in general, the known altered areas. The 1.3, 1.6 and 2.2 μm wavelength spectral data for Red Mountain were canonically transformed using a transformation which was empirically derived from discriminant function analysis of hydrothermally altered and unaltered materials in the Goldfield, Nevada region. A contour map was produced for the first canonical variable data. In general, the

contour map delineated the altered zones within the test area.

Multispectral reflectance imagery for the test area were obtained by NASA's 24-channel MSDS in the wavelength region of 0.4 to 12.5 μm. A false color ratio composite was produced by projecting the ratios 1.5/.82, 1.5/.46, .65/.46 in blue, green and red, respectively. These ratios were chosen after analysis of the field spectra, in order to provide the maximum differences between altered and unaltered materials. (Due to sensor malfunction, the 2.2 μm image was not available.)

Due to the heavy vegetation cover, Red Mountain appears green and yellow. Limonitic alteration on Red Mountain appears yellow in those areas which are less heavily vegetated. The northward shed alluvial fan composed of limonitically altered debris appears red on the imagery. The non-limonitic, silicically altered areas to the east of Red Mountain appear blue. All the altered areas are distinct in color with respect to both the unaltered areas and the heavily vegetated areas.

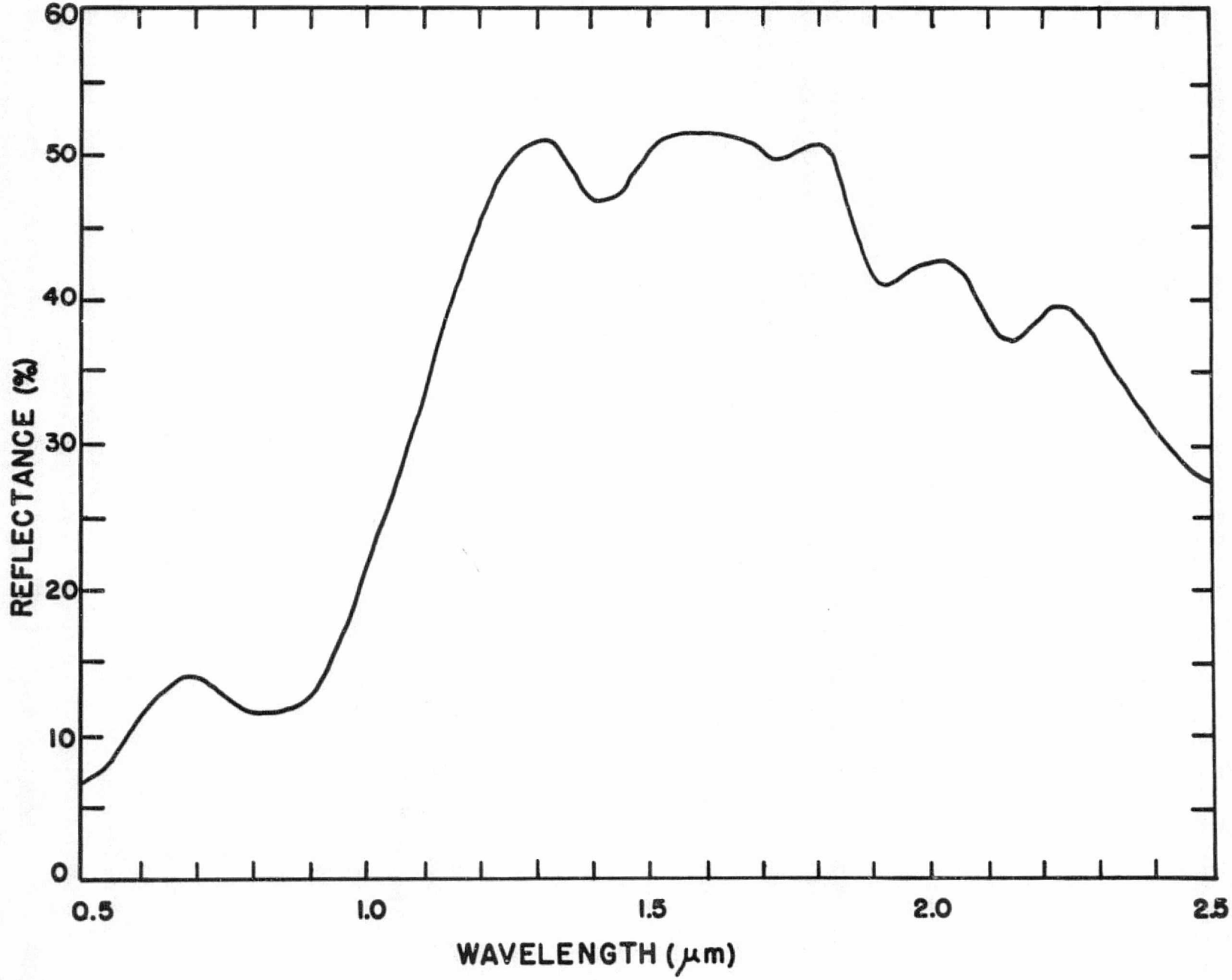

Figure 1. Spectral reflectance of altered material at Red Mtn., Arizona.

APPENDIX B

MAPPING OF HYDROTHERMAL ALTERATION IN THE CUPRITE MINING DISTRICT, NEVADA, USING AIRCRAFT SCANNER IMAGES FOR THE SPECTRAL REGION 0.46 TO 2.36 μm

Mapping of hydrothermal alteration in the Cuprite mining district, Nevada, using aircraft scanner images for the spectral region 0.46 to 2.36 μm

ABSTRACT

Color composites of Landsat Multispectral Scanner ratio images that display variations in the intensity of ferric-iron absorption bands are highly effective for mapping limonitic altered rocks but are ineffective for mapping nonlimonitic altered rocks. Analysis of 0.45- to 2.5-μm field and laboratory spectra shows that iron-deficient opalized rocks in the Cuprite mining district, Nevada, have an intense OH-absorption band near 2.2 μm, owing to their content of clay minerals and alunite, and that this spectral feature is absent or weak in adjacent unaltered tuff and basalt. Altered rocks in the district can be discriminated from unaltered rocks with few ambiguities by use of color-ratio composite images derived from multispectral (0.46 to 2.36 μm) aircraft data. In addition, some effects of mineralogical zoning can be discriminated within the altered area. Only variations in amounts of limonite can be discerned in shorter wavelength aircraft data, Landsat Multispectral Scanner bands, and color aerial photographs.

Michael J. Abrams
Jet Propulsion Laboratory
California Institute of Technology
Pasadena, California 91103
Roger P. Ashley
U.S. Geological Survey
Menlo Park, California 94025
Lawrence C. Rowan
U.S. Geological Survey
Reston, Virginia 22092
Alexander F. H. Goetz
Anne B. Kahle
Jet Propulsion Laboratory
California Institute of Technology
Pasadena, California 91103

INTRODUCTION

Exposed limonitic altered rocks can be discriminated from most unaltered rocks in computer-processed Landsat Multispectral Scanner (MSS) images (Rowan and others, 1974) because limonite, which is an important constituent of oxidized sulfide-bearing altered rocks, has a diagnostic spectral reflectance curve in the MSS response range (0.5 to 1.1 μm), owing to intense ferric-iron absorption bands. Although mapping altered rocks by this technique has considerable potential for augmenting conventional exploration methods in arid and semiarid regions, two important limitations have been recognized in south-central Nevada (Rowan and others, 1977): (1) nonlimonitic altered rocks, such as intensely leached silicified rocks, are not distinguishable from some silicic tuff and flow rocks, and (2) nonhydrothermally altered yet limonitic rocks, such as limonitic sedimentary, tuff, and lava flow rocks, are commonly not distinguishable from limonitic altered rocks. From the exploration point of view, the first limitation is probably more important because some altered, potentially mineralized areas might not be detected.

Analysis of 0.45- to 2.5-μm field and laboratory spectra of altered and unaltered rocks in south-central Nevada indicates that these limitations might be largely overcome by analysis of data in the 2.15- to 2.25-μm region, where nearly all altered rock spectra obtained exhibit an intense absorption band, referred to here as the 2.2-μm band. This band results from electronic processes associated with O-H bond stretching and Al-O-H bond bending vibrations in clay minerals, pyrophyllite, dioctahedral micas, and alunite (Hunt and others, 1971, 1973). The 2.2-μm absorption band is absent or weak in most unaltered rock spectra.

This report briefly describes evaluation of multispectral images obtained for the Cuprite, Nevada, mining district using the airborne Bendix 24-channel (MSDS) scanner. This site is a sparsely vegetated area consisting of intensely altered rocks that are not consistently distinguishable from unaltered rocks in Landsat enhanced images (Rowan and others, 1974, 1977).

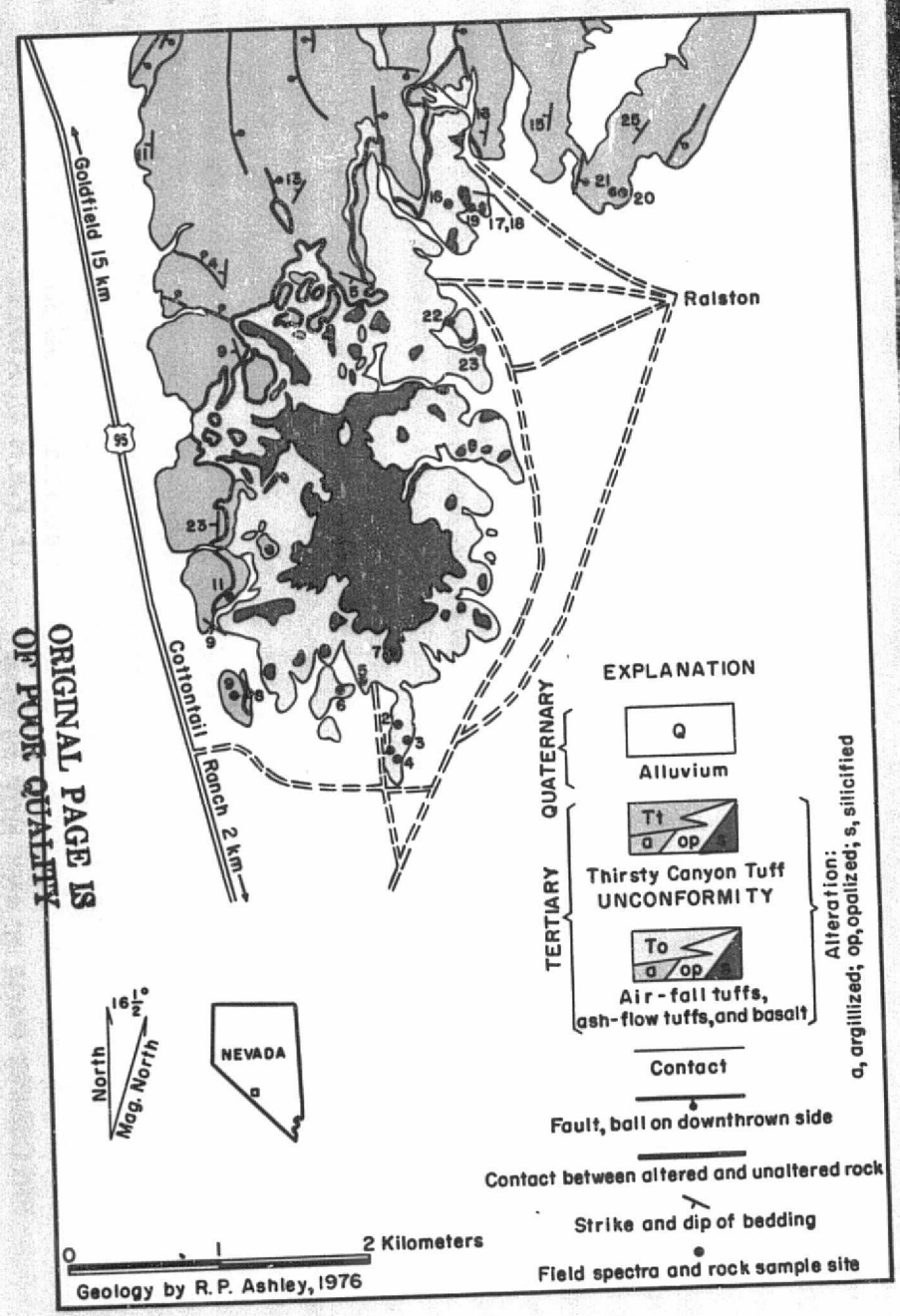

A

B

Figure 1. A. Simplified geologic map of Cuprite mining district, Nevada. B. Color-ratio composite using MSDS data: ratios 1.6/0.48 μm, 1.6/2.2 μm, and 0.6/1.0 μm displayed as green, red, and blue, respectively. C. Color air photo. D. Color-ratio composite using Landsat data: band ratios 4/5, 5/6, and 6/7 displayed as blue, green, and red, respectively.

GENERAL GEOLOGY

The Cuprite mining district (Fig. 1, A) includes exposures of hydrothermally altered rocks about 12 km² in extent, in two areas of approximately equal size. Minor sulfur, silica, and possible precious-metal production is attributed to the hydrothermally altered parts of the Cuprite district (Albers and Stewart, 1972). The eastern of the two altered areas is discussed here.

The older Tertiary unit (To in Fig. 1, A) is mostly hydrothermally altered; unaltered exposures occur along the northwestern and northern margins of the altered area and as a few isolated remnants within the altered area. This unit consists mainly of rhyolitic welded ash-flow and air-fall tuff, and basalt. The most extensive Tertiary unit, the Thirsty Canyon Tuff (Tt in Fig. 1, A), consists here of two soda rhyolite ash-flow cooling units, with an age of about 7 m.y. (Ashley and Silberman, 1976). Because this unit is in part hydrothermally altered, the alteration must have occurred less than 7 m.y. ago. The general geology is treated in more detail in Abrams and others (1977).

ALTERATION

The altered rocks are divided into three mappable units (Fig. 1, A): silicified rocks, opalized rocks, and argillized rocks. Silicified rocks are the most intensely altered rocks, and argillized rocks are the least intensely altered.

Silicified rocks, containing abundant hydrothermal quartz, form a large irregular patch extending from the middle to the south end of the area and also occur as scattered patches in the opalized rocks (Fig. 1, A). Opalized rocks contain abundant opal and as much as 30% to 40% alunite and kaolinite. Locally, an interval of soft, poorly exposed material mapped as argillized rock separates fresh rock from opalized rock. In the argillized rocks, plagioclase is altered to kaolinite, and glass is altered to opal and varying amounts of montmorillonite and kaolinite, but the other primary minerals are little affected. Clay is more abundant (more than 10%) than in most opalized rock samples.

Limonite content of most of the altered rocks is less than 5%, and large volumes of altered rocks are nearly limonite-free. Limonite is relatively abundant in the argillized rocks. Occurrences of relatively limonite-rich opalized rocks (some exceed 20% limonite) are spotty, but most are in the western part of the area. Silicified rocks commonly have at most only a few percent limonite; maximum limonite content is about 10%.

The altered rocks are free of significant desert varnish, except for silicified rocks that have developed a very vuggy and pockety weathered surface.

FIELD SPECTRAL MEASUREMENTS

Field spectral reflectance measurements and samples for petrographic analysis were obtained to guide the analysis of the multispectral scanner data. The field spectra (examples in Fig. 2) were acquired with the NASA Jet Propulsion Laboratory Portable Field Reflectance Spectrometer (PFRS) (Goetz and others, 1975), which measures the surface spectral reflectance in the wavelength region from 0.45 to 2.5 μm with moderate resolution

Unaltered Rocks. The Thirsty Canyon Tuff spectrum (typical devitrified ash-flow tuff, site 9, Fig. 1, A and B) is generally flat and lacks strong absorption features (Fig. 2). This is consistent with its mineral content, which is alkali feldspar and cristobalite with some tridymite and minor fine-grained hematite.

Altered Rocks. The spectrum of silicified material (site 7) shows a maximum at 1.7 μm and a weak absorption feature at 2.2 μm, which is manifested as a broad depression of the curve from 2.15 to 2.3 μm. This spectrum is consistent with the preponderance of quartz and small amounts of hydroxyl-bearing minerals. The presence of desert varnish on some of the samples analyzed results in depression of the entire spectral reflectance curve.

The spectrum of typical opalized rock shows a moderate rise in the visible region, a steep dropoff beyond 1.7 μm, and a deep 2.2-μm absorption band, produced in this case mainly by alunite. The lack of an absorption band at 0.85 μm reflects the absence of ferric minerals at this particular site. Other opalite samples display a wide variation in ferric mineral content but generally have notable amounts of hydroxyl-bearing minerals.

The argillized rock spectrum shows a strong absorption at 0.85 μm, a very steep rise from the visible to the infrared, and a moderately strong 2.2-μm absorption band. This reflects the presence of abundant red-orange hematite and moderate amounts of kaolinite.

IMAGE PROCESSING

The multispectral images were acquired from an altitude of 5,600 m above the ground, resulting in a maximum spatial resolution of approximately 10 m. All data were recorded in digital form.

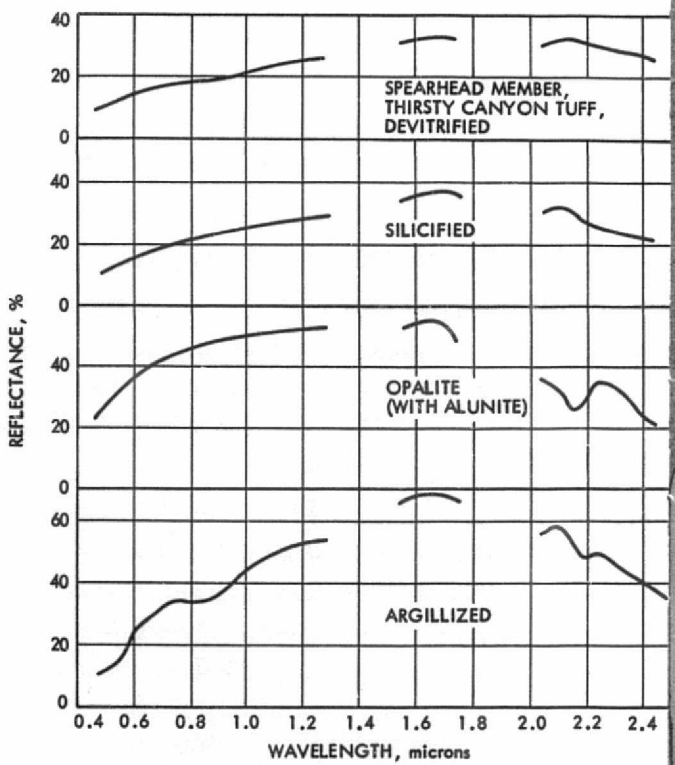

Figure 2. Representative spectral reflectance curves of altered and unaltered rocks at Cuprite mining district.

The Bendix scanner has 24 channels between 0.34 and 13.0 μm. The wavelength regions of the channels in the 0.4- to 2.5-μm region are 0.46 to 0.50, 0.53 to 0.57, 0.57 to 0.63, 0.64 to 0.68, 0.71 to 0.75, 0.76 to 0.80, 0.82 to 0.87, 0.97 to 1.05, 1.18 to 1.30, 1.52 to 1.73, and 2.10 to 2.36 μm.

Computer processing of the MSDS data involved characterizing and removing noise and removing major geometric distortions. No attempt was made to correct the data for atmospheric effects, and the lack of calibration data precluded conversion of the data to absolute radiances. Ratio values were contrast-stretched by applying a mathematical transformation to the values so that the dynamic range of the output image for each ratio matched the range of the film-recording medium. Any two or three film ratio images can be used to create a color-ratio composite image (CRC). Details of image-processing techniques have been described by Goetz and others (1975) and Soha and others (1976).

IMAGE INTERPRETATION

Color-Ratio Composite Derived from MSDS Data. The field spectra of the rock units exposed in the Cuprite district show which spectral bands and ratios are likely to be most effective for detecting ferric and hydroxyl-bearing minerals. Ratioing enhances differences in the shapes of spectral reflectance curves and suppresses brightness variations due to surface slope and albedo. We chose five bands and incorporated them in three ratios (values in microns) as follows: 1.6/2.2, 1.6/0.48, and 0.6/1.0 (the bands are designated by the approximate centers of the various scanner channels). The first ratio was chosen to delineate altered rocks having high reflectance near 1.6 μm relative to 2.2 μm, owing to the presence of hydroxyl-bearing minerals. The second ratio displays variations in surficial ferric iron content, with high ratio values indicating high concentrations. The third ratio was chosen to distinguish rocks with only moderately sloping spectra, including playa material, tuff, basalt, and bleached iron-deficient altered rocks (Fig. 2). Black-and-white film transparencies generated from these three ratios were combined into a CRC (Fig. 1, B) in a color-additive viewer. The red component represents the value of the ratio 1.6/2.2 μm, the green component the value of 1.6/0.48 μm, and the blue the value of 0.6/1.0 μm. The higher the value of each ratio, the higher the intensity of the corresponding color component.

A comparison of the geologic map (Fig. 1, A) and the CRC image derived from 24-channel scanner data (Fig. 1, B) indicates that the major altered and unaltered rock units can be distinguished in the CRC image. With field identification of the different units, it is possible to produce an alteration map quickly and accurately.

The silicified rocks (sites 7 and 18) appear dark red to brown and locally bluish purple to blue on the image, indicating that all three ratios are similar, with slight dominance of the 1.6/2.2-μm ratio over the other ratios. This is consistent with the mineralogy and the field spectra; 1.6/0.48 μm is low to moderate, whereas 0.6/1.0 μm and 1.6/2.2 μm are generally moderate but variable.

Opalized rocks range in color from magenta to red and yellow. All have large amounts of hydroxyl-bearing minerals, resulting in a very strong red component in the image. The variations in color are due to varying ferric mineral content. Where ferric iron is lacking (sites 1, 4, 16), the 0.6/1.0-μm ratio is moderately high, but 1.6/0.48 μm is very low, resulting in a significant blue contribution, which, when added to red, produces the magenta color seen in these areas (Fig. 1, B). As the limonite content increases, the slope of the spectral curve increases, resulting in higher values of 1.6/0.48 μm and lower values of 0.6/1.0 μm. In the image, this produces first red (sites 3, 19, 5) and then yellow (sites 2, 23, 6, 17) as the green component (1.6/0.48 μm) increases and the blue component (0.6/1.0 μm) decreases.

The argillized rocks (sites 11 and 8) on the west edge of the area are predominantly yellow-green, reflecting concentrations of both hydroxyl-bearing and ferric minerals. Where the argillized rocks appear green, they are partially covered by unaltered rock debris. This causes a reduction in the 1.6/2.2-μm ratio and hence less red contribution in the image.

Unaltered volcanic rocks and surficial material are dominantly dark green and blue to almost black in the CRC image and therefore readily distinguishable from the altered rocks. Much of the unaltered Thirsty Canyon Tuff appears nearly black on the image because all three ratios are relatively low, producing dark-gray tones in the black-and-white film transparency for each ratio and thus black or very dark colors on the CRC image.

Some additional details of MSDS image interpretation are discussed in Abrams and others (1977).

Comparison with Other Images. The color aerial photograph (Fig. 1, C) taken simultaneously with the scanner image (Fig. 1, B) shows the outline of the altered area well, because strongly bleached and/or hematitic altered rocks appear near the contact with unaltered rocks. The silicified rocks and parts of the opalized rocks, however, are gray and have albedos well within the range of albedos shown by the unaltered Thirsty Canyon Tuff, demonstrating that albedo is of limited value here, as in other areas (Rowan and others, 1974, 1977), for separating altered and unaltered rocks. Opalized rocks are distinguished easily from unaltered rocks and from most of the silicified rocks on the CRC. Silicified rocks and unaltered rocks are somewhat similar in both the photograph and the CRC but are more readily distinguishable in the CRC. Most limonitic areas in the scene are composed of hematite-bearing altered rocks that are partly surrounded by or adjacent to bleached areas. Thus, it is easy to infer from the color photograph that these hematitic areas are probably altered. Unaltered hematitic silicic tuff and flow rock and hematitic sandstone, however, often look exactly the same as hematitic altered rocks in color photographs, seriously limiting the value of photography where such rocks occur. This is demonstrated by comparison between sites 22 and 23, which are indistinguishable on the photograph but easily classified as probably unaltered (site 22) and definitely altered (site 23) on the CRC. Site 22 is unaltered rhyolite ash-flow tuff; site 23 is the same tuff altered to hematitic opalized rock.

As mentioned above, iron-poor rocks such as most of those at Cuprite are not consistently detectable in Landsat CRC images because the rocks lack diagnostic spectral features in the 0.5- to 1.1-μm wavelength region. Comparison of an enlarged Landsat color-additive CRC made using band ratios 4/5, 5/6, and 6/7 displayed as blue, green, and red, respectively (Fig. 1, D) with the geologic map (Fig. 1, A) shows that, in most places, both Thirsty Canyon Tuff and opalized and silicified rocks are represented by blue picture elements (pixels). Red pixels consist of limonitic rocks, including alluvium as well as altered bedrock.

Green pixels in the Landsat CRC do not appear to be consistently correlated with any particular rock unit.

SUMMARY AND CONCLUSIONS

Limonitic altered rocks having high albedo can be successfully detected and mapped using color aerial photographs and enhanced Landsat images, but limonite-poor altered rocks with variable albedo cannot. This study shows that additional spectral information between 1.1 and 2.5 μm provides a practical means for largely removing this limitation, because this region includes an absorption feature at 2.2 μm produced by any one of several important alteration minerals, including clay minerals, dioctahedral micas, pyrophyllite, and alunite. Multispectral data obtained by aircraft for the entire 0.4- to 2.5-μm spectral region provide many possibilities for creating useful enhanced images. Although the image presented here can probably be improved upon, it contains enough information to discriminate among zones within the altered area at the Cuprite mining district, as well as to discriminate between altered and unaltered rocks.

REFERENCES CITED

Abrams, M. J., Ashley, R. P., Rowan, L. C., Goetz, A.F.H., and Kahle, A. B., 1977, Use of imaging in the 0.46–2.36 μm spectral region for alteration mapping in the Cuprite mining district, Nevada: U.S. Geol. Survey Open-File Rept. 77-585, 19 p.

Albers, J. P., and Stewart, J. H., 1972, Geology and mineral deposits of Esmeralda County, Nevada: Nevada Bur. Mines and Geology Bull., v. 78, 80 p.

Ashley, R. P., and Silberman, M. L., 1976, Direct dating of mineralization at Goldfield, Nevada, by potassium-argon and fission-track methods: Econ. Geology, v. 71, p. 904–924.

Goetz, A.F.H., Billingsley, F. C., Gillespie, A. R., Abrams, M. J., Squires, R. L., Shoemaker, E. M., Lucchitta, I., and Elston, D. P., 1975, Application of ERTS images and image processing to regional geologic problems and geologic mapping in northern Arizona: NASA Jet Propulsion Lab. Tech. Rept. 32-1597, 188 p.

Hunt, G. R., Salisbury, J. W., and Lenhoff, C. J., 1971, Visible and near-infrared spectra of minerals and rocks—IV. Sulphides and sulphates: Modern Geology, v. 3, p. 1-14.

———1973, Visible and near-infrared spectra of minerals—VI. Additional silicates: Modern Geology, v. 4, p. 85-106.

Rowan, L. C., Wetlaufer, P. H., Goetz, A.F.H., Billingsley, F. C., and Stewart, J. H., 1974, Discrimination of rock types and detection of hydrothermally altered areas in south-central Nevada by the use of computer-enhanced ERTS images: U.S. Geol. Survey Prof. Paper 883, 35 p.

Rowan, L. C., Goetz, A.F.H., and Ashley, R. P., 1977, Discrimination of hydrothermally altered and unaltered rocks in visible and near infrared multispectral images: Geophysics, v. 42, p. 522–535.

Soha, J. M., Gillespie, A. R., Abrams, M. J., and Madura, D. P., 1976, Computer techniques for geological application, *in* Proceedings of Caltech/JPL Conference on Image Processing Technology, Data Sources, and Software for Commercial and Science Applications: Pasadena, Calif., NASA Jet Propulsion Lab.–California Inst. Technology JPL SP 43-30, p. 4-1–4-21.

ACKNOWLEDGMENTS

Reviewed by T. W. Offield and T. G. Theodore. This paper is the result of research carried out at the Jet Propulsion Laboratory, California Institute of Technology, under Contract NAS 7-100 sponsored by the National Aeronautics and Space Administration. Daryl Madura of the Jet Propulsion Laboratory's Image Processing Laboratory assisted with computer processing of the imagery.

MANUSCRIPT RECEIVED JULY 27, 1977

MANUSCRIPT ACCEPTED OCTOBER 7, 1977